Advances in Anticancer Protein Delivery Using Micro-/ Nanoparticles

**Wujin Sun**[a,b], **Yue Lu**[a,b], and **Zhen Gu**[a,b,*]

[a]Joint Department of Biomedical Engineering, University of North Carolina at Chapel Hill and North Carolina State University, Raleigh, NC, 27695, USA

[b]Center for Nanotechnology in Drug Delivery and Division of Molecular Pharmaceutics, UNC Eshelman School of Pharmacy, University of North Carolina at Chapel Hill, Chapel Hill, NC, 27599, USA

Abstract

Proteins exhibiting anticancer activities, especially those capable of discriminately killing cancer cells, have attracted increasing interest in developing protein-based anticancer therapeutics. This progress report surveys recent advances in delivering anticancer proteins directly to tumor tissue for inducing apoptosis/necrosis or indirectly to antigen presenting cells for provoking immune responses. Protein delivery carriers such as inorganic particles, lipid particles, polymeric particles, DNA/protein based biomacromolecular particles as well as cell based carriers are reviewed with comments on their advantages and limitations. Future challenges and opportunities are also discussed.

Graphical Abstract
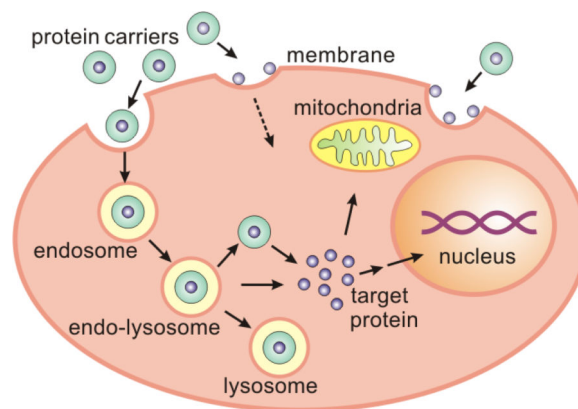
This progress report surveys recent advances in the development of micro-/ nanoparticles for delivering anticancer proteins to target cellular locus. Numerous types of proteins with anticancer activities and their relevant formulations, including inorganic materials, lipids, polymers, biomacromolecules and cells were summarized. Challenges and opportunities in this area were also discussed.

[*] zgu@email.unc.edu; zgu3@ncsu.edu.

1. Introduction

Cancer, the leading cause of death in the world, engendered over 10 million new cases each year.[1] Current therapies for cancer include surgery, radiation and chemotherapy, but they lack selectivity and cause severe damages to normal cells. Chemotherapy also suffers from severe multidrug resistance, repeated treatments enable tumors not only resistant to the chemotherapeutic agent used but also to agents belonging to the same family or even unrelated agents.[2, 3] In contrast, protein therapy shows highly specific set of functions and gained increasing use in clinical applications.[4] Proteins play important roles in all stages of cancer development by influencing cell morphology, adhesion, migration, cell-cell fusion and cancer-inducing virus invasion. Regulating protein activities can effectively affect tumor initiation, promotion and progression.[5] Proteins that regulate tumor cell life cycle can specifically inhibit tumor progression with minimal damage to normal cells.

Numerous proteins, such as cytokines, enzymes, antibodies and transcription factors have demonstrated anticancer activities[6, 7] and their action mechanisms can be classified into two categories: activating apoptosis signaling pathway or blocking growth signals.[8, 9] For example, tumor necrosis factor-related apoptosis-inducing ligand (TRAIL) is a cytokine released by normal cells and binds to the death receptors of tumor cells to initiate extrinsic apoptosis pathway.[10, 11] Cytochrome *c* is released from mitochondrion and initiates the intrinsic apoptosis pathway by activating caspases.[11, 12] The caspases are a family of proteases in the cytosol and they are the executioner of apoptosis signaling pathway that cleave protein substrates, leading to the characteristic apoptosis morphology.[13] Nucleases, such as DNAse I, that degrade DNA during apoptosis are also potent therapeutics against cancer.[14] Antibodies can kill cancer cells by specifically targeting oncogenic proteins or survival factors on tumor cell surface. For examples, CD20 antibody rituximab can ligate CD20 on B-cell surface and activate apoptosis signaling[15]; antagonists towards tyrosine kinases epidermal growth factor receptor (EGFR) and HER2 can block tumor proliferation activities.[16] Tumor suppressor p53 is a transcription factor that induces cell cycle arrest, apoptosis and senescence. While frequently mutated in cancer cells, its function can be restored by delivering wild type p53 into cancer cells.[17] Besides human derived proteins, some proteins derived from non-human sources also exhibit effective and selective cancer killing capability. For example, apoptin, a chicken anemia virus derived protein, can target to human tumor cell nucleus and induce apoptosis while remain in normal cell cytosome and exhibit no cytotoxicity.[18, 19] Asparaginase from *Escherichia coli* or *Erwinia chrysanthemi* is an enzyme that can deplete its substrate L-asparagine, an non-essential amino acid for most normal cells but essential for acute lymphoblastic leukemia cells, to arrest protein synthesis in leukemia cells and cause cell death.[20] Besides directly targeting tumor cells, proteins can also work as antigens to activate leukocytes, like T-cell, to treat cancer. After being phagocytized by antigen-presenting cell (APC), like dendritic cells, the protein antigens are processed and presented on APC cell surface to generate an antigen-specific cytotoxic T-lymphocytes (CTLs) response.[21, 22] CTLs are capable of recognizing tumor cells and inducing apoptosis.[23] Antigens like ovalbumin (OVA),[21, 23, 24] heat-shock proteins,[25] and interleukin-4/-12[26, 27] *et al.* were widely applied as antigenic protein in many formulations.

However, delivering protein is hampered by the intrinsic drawbacks of proteins, such as instability, large size and surface charges.[6] The delicate tertiary structures of proteins are easily denatured upon exposure to elevated temperatures and the peptide chains are susceptible to proteolytic or chemical degradations. Proteins losing activities often cause unexpected immune responses.[28] The large size of proteins prevented them from diffusing through plasma membrane and the electrostatic repulsion between most negatively charged proteins and cell membranes under physiological conditions further reduced protein uptake.[29]

Since the first FDA approved protein delivery therapy, PEGylated adenosine deaminase in 1990, nanocarriers for protein delivery developed rapidly in the last two decades.[30] The carriers include inorganic nanocarrers, lipid-based nanocarriers, polymeric nanocarriers, biomacromolecule based nanocarriers[6] as well as natural carriers like bacteria[31] and human cells[32-34] (**Figure 1**). The protein cargos can be loaded into the vectors either by covalent conjugation *via* chemical modification, peptide fusion *via* genetic recombination, physical adsorption through electrostatic/hydrophobic interactions or encapsulation *via* polymeric crosslinking.[6] Nanocarriers shield proteins from the denaturing biological environment and increase the circulation time of the cargo protein. Unique properties of tumor environment are the foundation for designing efficient protein delivery nanoparticles. When tumor size reaches >2 mm^3, increasing hypoxia of the local environment up-regulates the expression of pro-angiogenic proteins. New blood vessels will grow out of existing ones, namely angiogenesis, and blood vessels around tumor are aberrant in pericyte and basement membrane formation, leading to an enhanced permeability to particles within size range 20-200 nm. With the absence of lymphatic vessels, nanoparticles enter tumor tissue are retained. This phenomenon is named "Enhanced Permeability and Retention (EPR) effect". In addition, extracellular pH of tumor environment is slightly more acidic (pH 6.0-7.0) than normal tissue (pH 7.4), the differences in vasculature and pH of tumor environment have been widely utilized to design nanocarriers.[35] Targeting tumor tissues can be achieved either by passive targeting utilizing the EPR effect or by active targeting with conjugated ligands to bind receptors on target cells.[1] After nanocarrier accumulation in tumor tissue, efficient intra-cellular protein delivery also require efficient cellular uptake and endolysosomal escape. Delivery efficacy of the nanocarriers can be fine-tuned by adjusting particle size and surface properties.[37] After reaching the target locus, the cargo protein can be released either by passive diffusion or degradation of the nanocarrier.[30] By incorporating stimuli responsive moieties, like hydrolytically cleavable or photolabile linkers, into the nanocarreirs, spatial-, temporal- and dosage-controlled anticancer protein delivery can be achieved.[38]

Unlike nanoparticles that can be administered systematically for cancer targeting, micro-scaled polymeric particles easily clog capillaries, limiting their intravenous applications.[39] Thus, polymeric microparticles are generally administered locally at tumor site by subcutaneous injection for prolonged protein drug release.[40, 41] Despite the micro-scaled size of cell based microparticles, cell carriers like red blood cells are highly flexible and can circulate in the system for ~120 days to target reticuloendothelial system without clogging

the capillaries.[42] Properties like natural tropism, surface presented markers and high drug loading capacity render cellular carriers promising for protein delivery.[43]

In this progress report, we summarize recent advances in the design of micro-/nanocarriers for anticancer protein delivery. Advantages and limitations of currents particles as well as future opportunities and challenges are also discussed.

2. Inorganic nanocarriers for anticancer protein delivery

Inorganic carriers, such as calcium phosphate, carbon nanotube, graphene oxide, mesoporous silica nanoparticle and gold nanoparticle have been widely applied in drug delivery.[44] The core of inorganic nanoparticles retain their opticophysical[45] properties, making it suitable for formulating combined therapies or stimuli-responsive drug delivery systems.

2.1 Calcium phosphate nanoparticles

Calcium phosphate (CP) nanoparticle is a promising drug carrier for its high biocompatibility. It can be dissolved in endosome after cellular uptake into Ca^{2+} and PO_4^{3-}, which are main components of teeth and bones. Their size can be controlled by using different stabilizing agents.[46] Wu *et al.* used pyridoxial-5' phosphate functionalized CP nanoparticle to load RNAse (13.7 KDa) and asparaginase (150 KDa) *via* a pH sensitive aldimine linker between lysine residues of the protein and pyridoxial-5' phosphate. The carriers successfully delivered cargo proteins of different sizes into the cytosol of HeLa, HepG2 and L929 cells.[47] To develop orally administered anticancer drug, Kanwar *et al.* encapsulate lactoferrin, an anticancer protein derived from mammalinan milk, in CP nanoparticle. The lactoferrin loaded CP nanoparticle was further coated with alginate and chitosan to protect it from gastrointestinal tract degradation. The ~344 nm particle composed of a polymeric shell and an inorganic core transported the cargo protein across gut and mucosal surfaces into blood circulation and targeted it passively into human colon cancer cells in a Caco-2 xenografted mouse model.[48] CP nanoparticle was also developed for transcutaneous delivery of antigen by Perumal and coworkers.[49] Besides being the carrier, CP nanoparticle works as a vaccine adjuvant to enhance immuno-response as well. Negatively charged OVA and another vaccine adjuvant cellobiose were loaded onto the positively charged CP nanoparticle by adsorption. In a Balb/C mouse model with stratum corneum removed by tape-stripping, CP nanoparticle delivered OVA significantly enhanced the antibody titers.

2.2 carbon nanotubes

Carbon nanotubes (CNTs) are cylinders composed of single or multiple layers of graphene with carbon atoms bonded in hexagonal lattices.[50] Insolubility and cytotoxicity of pristine CNT hinder its biomedical application, which can be alleviated by functionalization. By functionalizing single wall carbon nanotube (SWCN) with poly (lactic-co-glycolic) acid (PLGA) to achieve high solubility and low cytotoxicity, Cheng *et al.* used PLGA-SWCN as a carrier to deliver caspase-3 into osteosarcoma cell MG-63. PLGA was degraded enzymatically after cellular internalization and released the conjugated caspase-3.[51] In

addition to polymers, proteins can be adsorbed onto CNT surfaces through van der Waals interactions and hydrophobic interactions to improve dispersability and bio-compatibility of CNTs.[52, 53] By adsorbing toxin ricin A chain protein (RTA) and a HER2 antibody non-covalently on multi-walled carbon nanotubes (MWNTs), Weng *et al.* selectively targeted HER2 receptors on specific breast cancer cells and delivered RTA to its natural intracellular locus to inhibit protein synthesis. [54] Further investigation of the uptake pathways in HeLa cells by tracking the a EGFP tag fused to RTA showed MWNT-RTA was internalized mainly through clathrin-mediated endocytosis (**Figure 2**).[55]

2.3 Graphene oxide nanosheets

Graphene is a 2-D material made of a single layer of carbon atoms, which were attached to each other by strong sp^2 hybridized carbon-carbon bond[56] The highly reactive surface of graphene makes it difficult to be suspended in solution, which can be overcome by oxidizing graphene into graphene oxide (GO). The oxidized portion of the surface offers functional groups for further conjugation and the un-modified part of the surface is capable of loading drugs through hydrophobic interactions and π–π stacking.[57] By conjugating six-armed poly-ethylene glycol (PEG) to the carboxyl groups of GO, Shen *et al.* improved the stability and biocompatibility of GO and used the PEG-GO as carrier for delivering RNase A and protein kinase A (PKA) to induce cell death and growth, respectively.[58] The RNAse A and PKA were loaded *via* π–π interactions between GO and proteins. Large surface area of GO leads to high loading capacity and the carrier also protected the proteins from proteolytic degradation. The cargo proteins were released *via* passive diffusion in a temperature dependent manner and intracellularly delivered proteins escaped endosomes and accumulated in the cytosol of HeLa cells. However, for the carbon based nanocarriers (CNT or graphene), a debate remained regarding the toxicity of these carriers that may hinder the application of these nanoparticles.[59]

2.4 Mesoporous silica nanoparticles

Mesoporous silica nanoparticles (MSNs) are mono-dispersed nanoparticles with controllable size and mesostructure.[60] MSNs have been widely used in delivering drugs and proteins for its ease of synthesis, versatile surface functionalization, high bio-compatibility and stability. Protein release can be controlled by tuning the size, shape and surface functionalization of MSN.[61] Mahony *et al.* modified MCM-41 mesoporous nanoparticle surface with amine (AM-41), which reversed the zeta-potential of the particle from negative to positive.[60] Positively charged amine modification increased OVA loading capacity of MCM-41 by 2.5-fold through electrostatic interaction. 7.9% of AM-41 loaded OVA were released within 30 min through passive diffusion. Besides being a carrier, the MSN also works as an adjuvant and elicited immune response at low OVA concentration. In addition to loading proteins by electrostatic interaction into MSNs, Gu *et al.* loaded cytochrome *c* into the channels of large pore-MSN by controlling the pore size of MSN with *N*,*N*-dimethylhexadecylamine.[62] To achieve controlled release of cytochrome *c* from MSN pores, Me dez *et al.* conjugated cytochrome *c* covalently into SH-functionalized MSN (MSN-SH) *via* disulfide bonds[63]. Cytochrome *c* was glycosylated with activated lactose (Lac$_4$) at lysine residues with a ratio of lactose/protein around 4/1 to increase the structural stability of cytochrome *c* during immobilization. The glycosylation protected cytochrome *c* from conformational disruptions

caused by the hydrophobic disulfide bond linker (SPDP) and it also prevented the modified cytochrome *c* from proteolytic degradation. The redox responsive release profile of cytochrome *c* from MSN-SH indicated 80% of the loaded cytochrome *c* was immobilized by covalent bonds. Confocal laser scanning microscope confirmed the redox responsive MSN-SPDP-Cyt *c*-Lac$_4$ was internalized into HeLa cells and it can escape the endosome to release cytochrome *c* into cytosol.

2.5 Gold nanoparticles

Gold nanoparticle has been widely applied in protein delivery due to its unique spectroscopic properties, ease of size control and facile surface functionalization.[64] Tang *et al.* utilized a peptide modified gold nanoparticles (HKRK-AuNP) as a stabilizer in the preparation of emulsion based nanoparticles (size 130-140 nm). Negatively charged anticancer protein caspase 3 was assembled onto the surface of the AuNP decorated nanoparticle, which contains an oil core for facilitated membrane fusion based protein delivery (**Figure 3**).[65] Ahn *et al.* utilized the immune adjuvant effect of AuNP to develop a vaccine for cancer immuno-therapy.[66] A tumor-associated antigen extra domain B (EDB) of fibronectin was loaded into AuNP to treat EDB-expressing tumors. Two cysteine residues were introduced into the N-terminus of EDB for conjugating EDB-OVA$_{257-269}$ into gold nanoparticle by Au-S bond. The conjugation increased the size of gold nanoparticle from 11.2 nm to 20 nm. AuNP conjugated EDB-OVA$_{257-269}$ induced 3-fold higher release of IFN-γ in dendritic cells and two fold higher release of IL-2 in OT-1 T cells than free EDB-OVA$_{257-269}$. *In vivo* test in a footpad of BALB/c mice showed the injected AuNP-EDB-OVA$_{257-269}$ were drained into lymph node and phagocytosed by lymph node resident dendritic cells, generating antigen-specific antibody. In a mouse model bearing a EDB-over expressing tumor 4T1, tumor growth was substantially inhibited by AuNP-EDB-OVA$_{257-269}$ (46%) than the free antigen (86%) and saline (100%). In addition to conjugating protein antigens onto AuNP covalently, AuNP can deliver protein without chemical interactions between the protein and AuNP. Due to its lipid-fluidizing capability, gold nanoparticle smaller than 10 nm is permeable to the skin, which can be utilized to deliver protein into deep skin layers.[67] Huang *et al.* synthesized 5 nm gold nanoparticle and tested its ability to deliver proteins percutaneously by co-administering the proteins with gold nanoparticle. Topical application of the gold nanoparticle transiently created openings in the skin, allowing the co-administered protein to penetrate. OVA was chosen as a model protein and its immune responses were tested in a Balb/c mouse model. The mixture of OVA and gold nanoparticle was highly immunogenic and generated anti-OVA IgG gradually over the time of immunization. In stead of utilizing the size of gold nanoparticles, Tang *et al.* utilized the photo-thermal properties of gold nanorod to ablate hydrophobic stratum corneum barrier of the skin and incubate OVA solution with the treated skin to deliver OVA.[68] The longitudinal surface plasma resonance of electrons in gold nanorod can be applied in photo-thermal therapy, which absorbs near-infrared light (NIR) between 800-900 nm. In the optimum NIR condition, continuous wave lasers at 150 mW increased skin temperature to 45 °C without denaturing skin surface proteins and translocated OVA efficiently into the skin. *In vivo* test showed that the OVA translocation efficiency by photothermal ablation of gold nanorod is comparable to that using a solid in oil dispersion. In addition,

immunochemistry analysis indicated that the phothothermal treatment of the skin also induced HSP 70 expession.

3. Lipid based carriers for anticancer protein delivery

3.1 Liposome

Liposomes are closed phospholipid bilayers containing an aqueous core, which can load water soluble drugs. Size of liposomes can be fine controlled by techniques like sonication, homogenization, extrusion or microfluidic mixing.[69] Modification of lipid components or surface of liposomes with different functional moieties enable facile surface modification of liposomes for desired drug loading and release properties. Yuba *et al.* developed a pH responsive liposome to deliver OVA.[24] Carboxylated poly(glycidol)s, pH sensitive polymers with high fusogenic properties, were synthesized and conjugated to the top of the head group of egg yolk phosphatidylcholine liposomes to introduce pH responsive fusognenic properties while avoid disrupting the stability of liposome. The carboxylate anion of the polymer enhanced liposome uptake by dendritic cell 2.4 by at least 5 fold and released OVA into dendritic cell cytosol to generate antigen-specific cytotoxic T lymphocyte. Mice immunized with the pH responsive fusogenic liposome containing OVA completely rejected OVA-expressing E.G7-OVA cells and achieved regression of E.G7-OVA tumors.

In addition to loading proteins in the aqueous core of liposomes, surface of liposomes can also be modified for protein loading. Sarker *et al.* explored the strategy of adsorbing negatively charged proteins to positively charged liposomes for functional protein delivery.[70] The synthetic lysine based cationic aminolipid with a trifluoroacetic acid counterion in the head group assembled into bilayered liposome with a size of 96 ± 40 nm and zeta potential of +60 mV at pH 7.4. Complexation of the positively charged liposome with the negatively charged proteins was achieved by mixing. They found that fetus bovine serum (FBS) proteins in the culture media readily exchanged with bovine serum albumin (BSA) adsorbed on liposome surface, and protein release rate is positively correlated with lipid content in the complex. Uptake and intracellular trafficking analysis showed that the uptake of the complex in HeLa cells is energy dependent and the complex can escape endosome entrapment after 24 h of incubation. Utilizing Ni^{2+}-His tag chelation, Miguel *et al.* incorporated a lipid nickel salt DOGS-NTA-Ni into liposome to tether TRAIL-His$_{10}$ onto liposome surface and obtained particles with z-average size of 178 ± 85.3 nm.[71] TRAIL bound to liposome surface increased the anticancer activity of free TRAIL in Jurkat leukemia T-cells by reducing the LC_{50} by around 14-fold. Using protein conjugated lipid component, Seifert *et al.* inserted anti-EGFR single-chain Fv fragment conjugated lipid with TRAIL conjugated lipid into a PEGylated liposome and enhanced the liposome's targeting efficiency towards EGFR-expressing Colo205 cells. Adding anti-EGFR single-chain Fv fragment reduced the EC_{50} of TRAIL loaded liposome from 20.2 ± 0.8 to $8.0 \pm 0.4 \mu M$ lipid.[72] Similarly, lipid particles without the aqueous core are also efficient carriers for intracellular protein delivery. For example, Kim *et al.* loaded cytochrome *c via* a conjugated lipophilic peptide into a 20-30 nm lipid nanodisc composed of lipid and apolipoprotein to induce apoptosis in H460 cells.[73] Wang et al. modified RNAse A or saporin with an acid-

labile *cis*-aconitic anhydride to make the protein surfaces negatively charged. The synthetic cationic lipids readily complexed with the modified protein through electrostatic interactions and formed ~130 nm nanoparticles.[74] The lipid-protein complex, but not protein or lipid alone, exhibited significant cytotoxicity towards B16F10 murine melanoma cancer cells.

Besides delivering protein as mono-therapy, liposome has been successfully applied in combination therapy for delivering a therapeutic protein together with a small molecule drug. Guo *et al.* encapsulated TRAIL and Doxorubicin (DOX) in the aqueous core of two liposomes, separately.[75] The delivered DOX selectively sensitized brain tumor glioblastoma multiforme (GBM) cells to TRAIL induced apoptosis by up-regulating DR5 and caspases −3, −8, −9 expression.[76] Instead of loading TRAIL and DOX in two separate liposome, Jiang *et al.* used a strategy to deliver TRAIL and DOX in one single polymeric gel coated liposome particle (Gelipo).[10] DOX is encapsulated in the aqueous core of a cell penetrating peptide modified liposome while TRAIL is adsorbed onto the hyaluronic acid (HA) shell *via* electrostatic interaction (**Figure 4**). The HA shell functions as a targeting ligand, which binds CD44 receptor of a variety of tumor cells, as well as a stimuli responsive element that can be degraded by hyaluronidase (HAase) rich in tumor environment. This strategy achieved sequential delivery of different cargos to different locations of the tumor cell. The TRAIL-DOX-Gelipo with a size of 110 nm accumulates at the tumor environment by both passive and active targeting. HAase at the tumor environment degraded the HA shell and released TRAIL to target death receptors on cell surface, the cell penetrating peptide on the remaining liposome surface then induced internalization of the DOX loaded liposome and delivered DOX intracellularly to cell nuclei. *In vitro* study showed that 80 % of the loaded TRAIL bound to cell surface in the presence of HAase and the presence of TRAIL on the outer-membrane of DOX-Gelipo reduced its IC_{50} towards MDA-MB-231 cell from 569 ng mL^{-1} to 83 ng mL^{-1} (in DOX concentration). *In vivo* study in a xenograft mouse model with implanted MDA-MB-231 tumors, Cy5.5 labeled TRAIL-Gelipo showed higher fluorescence signal at tumor site than normal tissue 48 h after injection, validating efficient tumor-targeting efficiency of this formulation.

3.2 Cell derived exosome/vesicles

In contrast with liposomes, which are biomimetic bi-layered lipid nanoparticle, cell derived exosomes or vesicles are the natural counterpart of liposome with huge potential in drug delivery.[77] These extracellular vesicles, with size ranging form 20 to 2000 nm, played important role in intercellular communication by transferring signaling molecules. Since exosomes are derived from endolysosomal pathway and vesicles are generating by budding from cell membrane, protein compositions on these microvesicle membranes are influenced by their parent cell lines.[78] Gehrmann *et al.* developed an anticancer immunotherapy by loading OVA and a glycolipid antigen α-galactosylceramide (αGC) into a dendritic cell derived exosome.[79] Supernatant of mouse bone marrow dendritic cell cultures pretreated with OVA, T-cell OVA-specific peptide SIINFEKL and/or αGC were used for exosome preparation by filtering through a 0.22-μm cut-off filter. While free αGC triggers invariant NKT (iNKT) anergy, αGC loaded in exosomes can activate iNKT cells, leading to the activation of NK and $\gamma\delta$ T cells with important anticancer activity, including OVA-specific CD8$^+$ T cells. In a mouse model with an OVA expressing melanoma, OVA/αGC loaded

exosome activated adaptive immunity without triggering iNKT cell anergy and decreased tumor growth. Similarly, Tian *et al.* challenged dendritic cells with exsosomes secreted from melanoma B16 and Lewis lung carcinoma (LLC) to present antigens and prepared exsosomes from these dendritic cells. The B16 and LLC antigen presenting exosomes effectively activated cytotoxic T lymphocytes and 70% and 87.5% of the immunized mice were tumor free at 30 days after B16 cell and LLC cell challenge, respectively.[80] To deliver proteins for anticancer pro-drug activation, Mizrak *et al.* expressed the protein/mRNA of a genetically fused protein CD-UPRT (cytosine deaminase fused with uracil phosphoribosyltransferase) in a donor HEK-293T cell, which can activate the co-administered pro-drug 5-fluorocytosine (5-FU) to its toxic form 5-fluoro-deoxyuridine monophos-phate (5-FdUMP) that can inhibit DNA synthesis.[81] Vesicles containing CD-UPRT protein/mRNA was harvested from the donor cell medium by differential centrifugation, ultracentrifugation, and filtration. Vesicles containing protein/mRNA of CD-UPRT was injected into a mouse model with pre-established nerve sheath tumors (schwannomas) followed by intraperitoneally administered 5-FC, the tumor growth was completely inhibited in 6 out of 9 mice.

4. Polymeric nanocarriers for anticancer protein delivery

4.1 Polymer-protein Conjugation

Covalent attachment of polymers, such as poly(ethylene glycol) (PEG), on protein surface is a facile and efficient strategy in delivering therapeutic proteins. The polymeric shell can shield the protein from its antigenic and immunogenic epitopes, protect it from phagocytosis or proteolytic degradation. By functionalizing PEG with specific functional groups at its terminal, PEG chains can be conjugated to reactive site groups, such as amine, thiol, caroboxyl or hydroxyl groups, on the protein surface.[82] With increased circulation lifetime and decreased dosage, many PEGylated protein therapeutics, such as enzymes, cytokines, antibodies and growth factors, were approved by FDA.[83] By conjugating PEG to protein surface lysine (NH$_2$) via a thioester, Chen *et al.* desinged a reversible protein PEGylation process in which the conjugated PEG can be removed at reducing environment.[84] Reactivity of the thioester can be modulated by changing the steric environment around the thioester to fit the glutathione (GSH) concentration difference between the intracellular environment (1-11 mM) and extracellular environment (2–10 μM). Using TRAIL as a model protein, PEGylated TRAIL showed reduced toxicity towards Jurkat acute T cell leukemia cell line but the toxicity was restored after removing PEG with GSH.

In addition to PEG, many other polymers have been applied in protein conjugation. For example, Murata *et al.* conjugated the cationic polymer polyethylenimine (PEI) to p53 *via* reversible disulfide bonds for enhanced endocytosis into cells through electrostatic interactions between the cationized protein and negatively charged cell membranes.[85] *E. coli* expressed p53 readily aggregated into inactive inclusion bodies, which was solubilized by PEI modification. The cationized p53 was internalized by Saos-2 cells in denatured form and refolded into active tetramers after entering the reductive intracellular environment, upregulating p53 targeted protein p21/waf1 to induce apoptosis. Keefe *et al.* utilized a zwitterionic polymer poly(carboxybetaine) (pCB) to conjugate a model protein *α-*

chymotrypsin.[86] Zwitterionic polymers are polyelectrolytes that can pose a strong ionic interaction with water *via* their positively and negatively charged groups. Unlike PEG, increase in protein stability is not related with pCB molecular weight or the number of pCB chains per protein. Without posing a PEG like steric hindrance between substrate and its binding pocket, the attachment of pCB drew water away from the protein hydrophobic center, allowing substrate to interact with its binding site. Ding *et al.* applied polymalic acid (PMLA), a natural polymer synthesized by *Physarum polycephalum* as a carrier for anticancer protein delivery.[87] A recombinant protein that fused cytokine interleukin-2 (IL-2) with an antibody specific for human HER2/*neu* was conjugated to PMLA. They demonstrated that the nanobioconjugate is capable of retaining the biological activity of IL-2 and target HER2/neu-positive tumor cells to inhibit their growth.

4.2 Crosslinking based encapsulation

In solution based polymerization, free proteins were dissolved with monomers or polymers in the same solution, into which the addition of cross-linkers and/or initiators lead to the encapsulation of proteins in polymeric nanogels. Gu *et al.* encapsulated caspase-3 in a cocoon like polymeric capsule non-covalently by *in situ* polymerization on the surface of caspase-3 (**Figure 5**).[88] Monomers, such as acrylamide (AAm) and *N*-(3-aminopropyl) methacrylamide (APMAAm), together with a cross-linker adsorbs onto protein surface *via* electrostatic interactions or van der Waals force, the addition of radical initiators into the monomer-protein solution starts the polymerization immediately. At the molar ratio of protein/AAm at 1200, size of capase-3 increased 5 nm to 13 nm after the encapsulation. The positively charged monomer APMAAm reversed the surface charge of caspase-3 from negative to positive for efficient cell penetration. By tuning the property of the cross-linker, protein release behavior can be controlled. Using a bisacrylated cross-linker that contains the substrate peptide of caspase-3 (VDEVDTK), a self-degradable protein nanocapsule was obtained. With a non-degradable cross-linker as control, the researchers demonstrated that the degradable capsule induced HeLa cell apoptosis within 24 h while no sign of apoptosis was observed with naked caspase-3 or caspase-3 encapsulated with non-degradable cross-linker. To control the degradation process spatiotemporally, the researchers modified the aspartic acid of the cross-linker with a photolabile *o*-nitrobenzyl ester moiety to protect the peptide form degradation. In the optimum condition with UV radiation for 40 s, the photolabile moiety dissociated from the peptide linker and exposed the cross-linker for caspase-3 degradation, releasing the encapsulated caspase-3. Using the same strategy but with caspase-3 degrading the capsule from outside, a fluorescent single protein nanocapsule for caspase-3 activity assay was developed.[89] Based on these work, Biswas *et al.* used a bisacrylated peptide linker that contained the peptide substrate of furin, an endoprotease ubiquitously expressed in many mammalian cells.[90] Instead of releasing the encapsulate protein from within, furin can degrade the capsule and release the cargo protein externally to deliver them to their corresponding nuclear and cytosol location. Researchers from the same group also developed a redox responsive cross-linker that contained a disulfide bond.[29] Anticancer proteins, whether monomeric caspase-3 (30 KDa) [29] or apoptin complex (2.4 MDa)[19], were successfully delivered intracellularly, where the high GSH concentration triggered the capsule degradation and protein release. Intracellular trafficking of rhodomine-labeled apoptin encapsulated in the redox responsive nanocapsule by CLSM analysis

showed that the delivered apoptin localized only in the nucleus of cancer cell to induce apoptosis but remained in the cytosol of normal cells.

In addition to covalent cross-linking, ionic cross-linkers that binds oppositely charged polymers were also used in preparing protein loaded nanoparticles. By adding negatively charged cross-linker sodium tripolyphosphate to a chitosan solution containing OVA or melanocyte-associated antigen gp100 protein, Li *et al.* obtained antigen loaded chitosan nanoparticles.[91] The chitosan nanoparticle has a size of 258 ± 15 nm and zeta potential of 27.6 ± 4.7 mV when loaded with OVA. The OVA loaded chitosan nanoparticle induced significant higher anti-OVA IgG than OVA solution in both intact and stratum corneum-removed skin. In BALB/c mice models inoculated with B16BL6 cells, chitosan nanoparticle loaded with gp100 increased the survival rate from 20% to 80 % after 20 days of inoculation.

4.3 Emulsion based encapsulation

In emulsion polymerization based encapsulation, the particles are morphed by interfacial repulsion between the aqueous phase and the organic phase. Various bio-degradable polymeric carriers for functional protein delivery were prepared by emulsion techniques. Noh *et al.* prepared a theranostic PLGA nanoparticle delivering both antigen (OVA) and bimodal imaging probes (indocyanine green (ICG) and iron oxide).[92] The multifunctional polymeric nanoparticle (MPN) can trace the migrations of MPN internalized dendritic cells into lymph nodes. The MPN was prepared by the double-emulsion solvent extraction method, in which the aqueous ICG-OVA solution was homogenized in an organic phase of methylene chloride containing PLGA and iron oxide to obtain a water in oil (w/o) emulsion. Then the w/o emulsion was emulsified in a second aqueous phase (PVA solution) by sonication to produce a w/o/w emulsion followed by solvent evaporation to harden the PLGA particles. The MPN has a smooth surface morphology with an average diameter of 189.57 ± 32.89 nm and zeta potential around - 23 mV. Study of MPN-OVA intracellular trafficking in dendritic cell by fluorescent microscope showed that FITC labeled OVA can be detected in the lysosome and co-localization of FITC-OVA with ICG in the cytosol can be observed. Lymphocytes isolated from the treated mice showed high cytotoxicity towards EG7-OVA cells, while low cytotoxic lymphocyte was detected with mice treated with soluble OVA or human serum albumin loaded MPN. Similarly, Sarti *et al.* encapsulated OVA and a immunostimulant monophosphoryl lipid A (MPLA) in a 320 nm PLGA nanoparticle for oral antigen delivery.[93] In addition to PLGA nanoparticles, PLGA microparticles can also be prepared *via* double emulsion. Kim *et al.* encapsulated PEGylated TRAIL in PLGA microsphere for sustained local release at tumor sites.[40] The PEG-OVA loaded microsphere has a size of 12.9 ± 1.98 μm. PEGylation at N-terminal of TRAIL significantly enhanced its encapsulation efficiency as well as anticancer efficiency possibly due to the shielding effect of PEG on protein surface. *In vivo* study with BALB/c athymic mice bearing HCT 116 tumors showed 78.3 % tumor suppression with PEGylated TRAIL microsphere while only 25.9 % tumor suppression was observed with TRAIL microsphere at 24 days. In stead of double emulsion, Azagarsamy *et al.* demonstrated a photo-degradable protein delivery carrier synthesized by inverse emulsion. [94] The cargo protein was dissolved in the aqueous phase containing monomer hydroxyethylacrylate (HEA) and a light sensitive cross-linker.

Followed by dispersion in the organic phase of n-heptane containing surfactant Brij 30, the polymerization was initiated by adding radicals into the organic phase. The obtained 25-40 nm nonoparticles showed continuous decrease in size upon light irradiation (λ=365 nm).

4.4 Dendrimers

Unlike linear polymers, dendrimers are hyperbranched polymers characteristic for their monodispersity, nanometric size range, controllable architecture and surface groups. Dendrimers generally contain three distinct domains: a multifunctional core, branched repeats emanating from the core with radically concentric layers called "generations" and surface functional groups at the terminal of the branches.[95] Sheng *et al.* developed a mannosylated polyamidoamine (PAMAM) dendrimer for OVA delivery.[96] A generation 4 cystamine dendrimer containing 64 amine sites was mannosylated with 30-fold molar excess of activated mannose. Reducing the dendrimer core exposed a thiol group for OVA conjugation. Mannosylation enhanced the uptake efficiency of the dendrimer loading OVA *via* its interaction with mannose receptors on antigen presenting cell surface. The Mannosylated dendrimer loading OVA (MDO) not only enhanced antigen presentation but also induced dendritic cell maturation. Mice pre-immunized with MDO showed high resistance to B16-OVA tumor cells with delayed onset, slower kinetics of growth and higher survival rate. Ng *et al.* conceived a reversible pH responsive protein delivery strategy using second generation PAMAM dendritic shell to coat the surface of therapeutic proteins (**Figure 6**).[97] After modifying lysine residues on protein surface with 4-carboxyphenylboronic acid and modifying PAMAM dendron core with ethynyl hydroxamic acid, the dendrons self assembled onto protein surfaces *via* an acid labile boronic acid/salicyl hydroxamate ligation. Enzymatic activities were sterically blocked by the branched dendrons with high volume weight ratio at physiological pH (pH 7.4). The drendritic shell facilitated clathrin-dependent endocytosis of the cargo protein and escaped the endosome by proton sponge effect. Degradation of the shell under acidic environment (pH 5.0) can restore enzyme activities by > 90 %. In stead of directly ligating proteins onto dendrimers, Ng *et al.* also developed a multidomain protein delivery system that used protein streptavidin as the multi-functional core to assemble biotinylated proteins (p53 or cytochrome *c*) and second generation PAMAM dendrons.[98] The PAMAM dendrons presented positively charged surfaces for enhanced cellular uptake and increased the size of unmodified streptavidin from ~ 4 nm to ~ 5 nm. Further assembly of biotinylated p53 or cytochrome *c* increased the sizes further to 7.53±1.35 nm and 7.06±1.15 nm, respectivley. The uptake efficiency of the nanocomplex is considerably affected by the molar ratio of PAMAM dendron to the loaded protein, 40-fold molar excess of the dendron achieved the maximum p53 delivery efficiency to the cytosol of HeLa cells *via* endocytosis. P53 delivered into SaOS cells by the nanocomplex activated the apoptosis pathways and upregulated caspase −3, −7 activities.

4.5 Polymersome

Similar to liposome, polymersomes are hollow spheres with an aqueous core enclosed by membranes. The hydrophobic middle part of the membrane can integrate hydrophobic drugs while the hydrophilic core can encapsulate water soluble drugs, nucleotides or proteins. Instead of lipids, polymersomes are made of amphiphilic block copolymers that can be manipulated with different stability and permeability to control drug release.[99] Based on

the link between an oxidative endosomal environment in dendritic cells and their antigen cross-presentation capability, Scott *et al.* applied a 100 nm oxidation-sensitive polymersome self-assembled from a block copolymer poly (ethylene glycol)-bl-poly(propylene sulfide) (PEG-PPS) to deliver OVA and small molecule adjuvants.[100] Oxidation of PPS into sulfoxide restructured the polymersome vesicle into micelles, releasing the encapsulated cargos, and the protein release kinetics were affected by oxidative stress. While no release was detected with 0.1% hydrogen peroxide within 48 h, 75 % of the encapsulated protein was released within 24 h at the presence of 0.5% hydrogen peroxide. The dissociated amphiphile fragments permeabilized endosome membrane to allow endosomal escape and the resulting micelle possessed a hydrodynamic size of 50 nm, which was small enough to be cleared out of the body by kidney.

In contrast to using the oxidative stress within dendritic cells, Wang *et al.* utilized the reductive endosomal environment of Hepatoma cells and designed a redox responsive chimeric polymersome.[101] Three polymeric blocks, the hydrophilic PEG, the hydrophobic poly(*ε*-caprolactone) (PCL) and the positively charged poly(2-(diethylamino)ethyl meth-acrylate) (PDEA) were assembled with different functional moieties, such as galactose (Gal) and disulfide bonds (SS), into PEG-PCL-PDEA, Gal-PEG-PCL, and PEG-SS-PCL. With PEG-PCL-PDEA as the polymersome backbone, Gal-PEG-PCL and PEG-SS-PCL were intercalated into the asymmetric polymersome to introduce a targeting ligand and a reduction responsive moiety, respectively. With positively charged PDEA locating in the interior of the polymersome, high protein loading capacity was achieved *via* electrostatic and hydrogen bond interactions. Protein release was significantly accelerated in the presence of 10 mM GSH, with 77.2 % and 22.1% of FITC-BSA released from the polymersome (50 % PES-SS-PLC) at 37 °C within 12 h in the presence and absence of GSH, respectively. Granzyme B delivered into HepG2 cells using this chimeric polymersome showed a markedly low IC_{50} of 2.7 nM, which is comparable to microinjected granzyme B into MCF-7 cells.

In addition to single stimulus responsive polymersomes, dual stimuli responsive polymersomes were also developed for intracellular protein delivery. Cheng *et al.* developed a reduction and temperature dual-responsive polymersome for intracellular protein delivery.[102] Thermo-sensitive triblock copolymes made of PEG, poly (acrylic acid) (PAA) and poly *N*-Isopropylacrylamide (PNIPAM) were synthesized with lower critical solution temperatures (LCST) of 38-39 °C under physiological conditions. The triblock copolymer PEG-PAA-PNIPAM readily assembled into stable polymersome at elevated temperatures, which was further crosslinked with cystamine to make it stable at physiological temperature. Exposure of the polymersome to both physiological temperature and highly reducing environment simultaneously triggered the release of the encapsulated OVA or cytochrome *c*.

4.6 Micelles

Self-assembled from amphiphilic block copolymers but without the aqueous core as in polymersomes, micelles also have core-shell structures that can be applied in drug delivery.[103] Lee et al. applied a polyionic complex (PIC) micelles assembled from a block copolymer with a neutral block (PEG) and a positively charged poly amino acid block to

deliver positively charged protein cytochrome *c*.[104] To enhanced the stability of PIC micelles for protein delivery, lysine residues of cytochrome *c* was modified with citraconic amide and *cis*-aconitic amide to convert the surface charge from negative to positive as well as increased charge density. Moreover, pH sensitivity of the formulation was endowed by the pH labile amide groups on the surface of cytochrome *c*, which could shed from cytochrome *c* and expose the negatively charged surface to destabilize the micelle (**Figure 7**). Ren *et al.* reported a pH/sugar responsive PIC core-shell micelle assembled from two block copolymers.[105] A neutral block (PEG) and an ionic block (negative poly-glutamic acid (PGlu) or positive poly-lysine (PLys)) were incorporated into the copolymers to assemble the micelle through electrostatic interactions. Phenylboronic acid and catechol were incorporated into the PGlu and PLys blocks, respectively, to crosslink the ionic core by boronate ester bonds. The crosslinking reduced the size of micelle from 172.5 nm to 85.3 nm, and increased the zeta potential from -0.21 ± 1.56 mV to 2.32 ± 1.68 mV (35% crosslinking ratio). Proteins with either positive or negative charges were successfully encapsulated in the micelle core *via* electrostatic interactions in neutral aqueous conditions. Due to the dual responsiveness of the boronic ester bond to competing diols or acidic pH, cross-linked PIC micelle was stable under physiological conditions but disassembled in the presence of excess fructose or endosomal pH to release the loaded cargo. Cytochrome *c* loaded in this cross-linked PIC micelle showed minimal release (<20%) in a stimuli-free environment within 24 h. The presence of 50 mg/mL fructose, but not glucose, induced the release to ~50 % during the same time, which was further augmented by changing the environment pH from 7.4 to 5.0. Uptake of the cytochrome *c* loaded micelle could be observed in HepG2 cells within 4 h and it induced much higher apoptosis (17.55%) than free cytochrome *c* (6.66%) within 24 h.

Unlike the ionic core formed by electrostatic interaction, Keller *et al.* synthesized a pH responsive micelle with a core formed by hydrophobic interactions.[106] The amphiphilic copolymer was synthesized by Reversible Addition-Fragmentation Chain Transfer (RAFT) polymerization with a hydrophilic block containing *N*-(2-hydroxypropyl) methacrylamide to form the micelle shell and a hydrophobic block containing dimethylaminoethyl methacrylate, propylacrylic acid, and butyl methacrylate to form the core. Pyridyl disulfide groups were incorporated into the hydrophilic shell for reversible antigen conjugation while the pH responsive core can disintegrate the 30 nm micelle into < 10 nm particles at pH 5.8 and destabilize endosomal membrane for endosomal escape. *In vitro* tests with dendritic cell 2.4 showed that OVA conjugated to the micelle surface generated 67-fold higher antigen than soluble OVA within 4 h after uptake. C57Bl/6 mice subcutaneously immunized with OVA conjugated micelle showed that the micelles were drained into the lymph nodes and preferentially associated with dendritic cells after 24 h of injection, activating OVA-specific CD8+ T cells.

5. Biomacromolecules for anticancer protein delivery

5.1 DNA nanostructure

With superior biocompatibility and programmability, DNA nanostructures, from simple linear chains to complex three dimensional structures, were explored as carriers for

therapeutic protein delivery. Zhang *et al.* reported a multivalent polymeric DNA scaffold synthesized by rolling circle amplification for antibody conjugation.[107] With a circular ssDNA as template, long chain ssDNA containing repeated sequences complementary to the template was amplified using a oligonucleotide primer and phi 29 DNA polymerase. Biotin modified dUTP was incorporated into the ssDNA product for complexing with biotinylated anti-CD 20 *via* NeutrAvidin as the adaptor. This cluster of anti-CD20 ligated cancer cell surface CD20, initiating a signaling cascade to induce apoptosis. The anti-CD20 cluster showed significantly higher anticancer activity towards B-cell cancer cells than soluble anti-CD20.

Liu *et al.* developed a protein antigen delivery platform using a DNA tetrahedron based on Watson-Crick base pairing.[108] DNA oligos with precisely designed complementary and linker sequences were hybridized *via* temperature dependent DNA denaturation and annealing. With a biotin moiety incorporated into one of the oligos, streptavidin was conjugated into the tetrahedron as a model antigen together with a oligonucleotide adjuvant CpG. The cellular internalization efficiency of DNA tetrahedron was tested in mouse macrophage-like cell line RAW 264.7, which showed co-localization of the antigen loaded tetrahedron with lysosome within 2 h. Analysis of antibody induction efficiency of the DNA tetrahedron delivered antigen in a BALB/c mouse showed long term immunity responses, possibly due to its activation of antigen-specific memory B cells. Using a similar structure, Erben *et al.* filled the 2.6 nm central cavity of a DNA tetrahedron, which could contain a roughly 60 KDa globular protein, with cytochrome c (12.4 KDa) by conjugating amine groups on cytochrome c surface to 5' of the DNA oligo before assembling the tetrahedron.[109]

Douglas *et al.* designed an aptamer gated DNA nanorobot for antibody delivery (**Figure 8**).[110] The nanorobot was assembled by folding a 7308 bp filamentous phage derived ssDNA scaffold with hundreds of short DNA oligo staples into customized three dimensional structure. Antibodies were conjugated to the 5' end of a 15 bp ssDNA linker for hybridizing onto the interior surface containing extended staples as payload binding site. Two of three DNA aptamer based locks, which can be opened with specific antigen keys on specific cell surface, were incorporated into the barrel like nanorobot simultaneously to control the sequester and exposure of the loaded payload. Selected combination of the payload antibodies and aptamer locks can regulate specific cell functionalities in targeted cell lines, such as inhibited aggressive natural killer cells or activated T cells.

5.2 Protein nanoparticle

Although cell membranes are impermeable to most proteins, self-assembled protein cages or proteins fused with a cell penetrating peptide or antibody are readily internalized by mammalian cells. Cell penetrating peptide (CPP), which can be classified into cationic, amphipathic and hydrophobic, interacts with various cell surface molecules to deliver the tethered protein *via* multiple pathways, including direct translocation through membrane bilayers and endocytosis.[111] Granadillo *et al.* used a cell penetrating and immunostimulatory peptide derived from the Limulus polyphemus protein (LALF$_{32-51}$) to deliver human papillomavirus (HPV) 16 E7 antigen for cancer immunotherapy.[112]

Immunofluorescence microscopy with J774 murine macrophages cell line confirmed the cell penetrating ability of $LALF_{32-51}$-E7 by the detectable fluorescence signal after incubation for 30 min while no signal was detected with soluble E7. C57BL/6 mice inoculated with TC-1 tumors showed statistically significant reduction in tumor size only with $LALF_{32-51}$-E7 vaccination but not with $LALF_{32-51}$, E7 or their mixture. Essafi *et al.* genetically fused a protein transduction domain of HIV transactivating transcription factor protein (TAT) with transcription factor FOXO3 to treat leukemia.[113] FOXO3 could induce cell cycle arrest in lymphocytes but Akt-dependent phosphorylation of wild type FOXO3 excluded FOXO3 from the nucleus and inhibited its transcriptional activity, which was avoided by mutating the phosphorylation sites of wild type FOXO3. The TAT fusion delivered both wild type and mutant FOXO3 into the cytosol of Jurkat cells but only the mutant FOXO3 was successfully targeted to the nucleus. Flow cytometry analysis showed that TAT fused mutant FOXO3 induced massive cell death in Jurkat T-cell leukemia and K562 chronic myelogenous leukemia cells.

Antibodies can deliver cytotoxic agents, including proteins, radionuclide and small molecules, into malignant cells by targeting overexpressed receptors on cell surface.[114] Bull-Hansen *et al.* targeted human epidermal growth factor receptor HER2, which is overexpressed in 20% - 30% of breast tumors, with HER2 single-chain antibody fragment MH3-B1 fused type I RIP toxin gelonin (rGel).[115] Tests in four breast cancer cell lines with different HER2 expression levels (MDA-MB-231, BT-20, Zr-75-1 and SK-BR-3) showed that ~120 times more MH3-B1/rGel accumulated in HER2 high expressing cell line SK-BR-3 than HER2 low expressing cell line MDA-MB-231 and the IC_{50} was reduced by ~1000 time in SK-BR-3 while no obvious difference in IC_{50} was observed between rGel and MH3-B1/rGel in MDA-MB-231. Despite the compelling targeting efficiency of anti-body conjugated proteins, lacking a cost-effective production platform hurdled its translation to marketplace. To solve this problem, Tran *et al.* used the chloroplast of green alga *Chlamydomonas reinhardtii*as instead of commonly used *E. coli* or CHO cells as a platform to express an anti-body fused exotoxin A, which can target B-cell surface receptor CD22 and inhibit protein translation in B-cell tumors.[116] The algae contains a single chloroplast with machineries like chaperons, protein disulfide isomerases and peptidylprolyl isomerases to fold and assemble complex eukaryotic proteins. Monomeric CD22 antibody fused exotoxin A synthesized by the chloroplast selectively killed CD22 expressing B cells like CA-46 and Ramos with IC_{50} of 0.246 nM and 1.39 nM, respectively, but it did not inhibit CD22 deficient Jurkat T-cell proliferation. The authors reasoned that with algae's potential as cost-effective source of bio-fuels, it holds great promise to function as a cost-effective platform for producing protein therapeutics.

Protein nanocages, such as ferritin, heat shock protein or virus capsid, are mono-dispersed symmetrical assemblies of a certain number of protein subunits. The highly defined structure and biocompatibility of protein nanocages make them promising platforms for drug delivery.[117] Patel *et al.* synthesized bacteriophage MS2 and Qβ virus like particles (VLP) that were symmetrical icosahedrons by cell free protein synthesis as a platform to deliver proteins and nucleotides.[118] Functionalized cargo molecules were covalently conjugated on the surface of the VLPs containing non-natural amino acids as binding site. The non-natural amino acids were analogous to methionine but contained terminal azide and alkyne groups

for click chemistry based coupling. In contrast to surface conjugated cargo loading, Wörsdörfer *et al.* encapsulated a toxic HIV protease in the void core of a protein capsid by directed evolution.[119] The evolved lumazine synthase self-assembled into icosahedral capsids, containing negatively charged residues on luminal surface to enhance its interaction with the positively charged guest molecules.

6. Living particles for anticancer protein delivery

6.1 Bacteria

Advances in synthetic biology have made it easy to manipulate bacteria genetics to construct nano-/micro- scale factories producing therapeutic molecules. Advantages like targeting specificity, self-propulsion and environment sensing capabilities made bacteria a promising carrier for cancer therapy.[120]

Zhu *et al.* utilized rod shaped *E. coli* (1-3 μm in length and 0.5μm in diameter) as carrier for controlled protein delivery.[121] The non-invasive *E. coli* strain BL21, a model protein expression host in the field of biotechnology, was used to deliver exotoxin A by expressing it from plasmid pET28a. To facilitate protein release, a red-emissive cationic polyelectrolyte was coated onto BL21 (BL21 capsule) together with pretreating BL21 with membrane disrupting peptide antibiotic polymyxin B. Polyelectrolyte coating collapsed the smooth surface of BL21 and confocal laser scanning microscopy confirmed that the BL21 capsule was internalized by A 498 human kidney carcinoma cells and located around the nucleus. MTT assay with A498 cells showed that only the exotoxin A expressing BL21 capsule caused severe cell death (~ 50%) within 48 h while the empty BL21 kept a 100 % cell viability and empty BL21 capsule caused only slight cell damage (> 80 % viability). In addition, the author noted that the coated polyelectrolyte can also generate reactive oxygen species upon light triggering, making the polyelectrolyte coated BL21 a versatile vector for tumor destruction.

Instead of using cell membrane disrupting agents to facilitate protein release, Gouëllec *et al.* utilized the needle-like type III secretion system (T3SS) of *Pseudomonas aeruginosa* (*P. aeruginosa*) for antigen delivery.[122] *P. aeruginosa* was genetically engineered for attenuated virulence by deleting the genes coding exonucleotidse A and B subunits, which disabled *P. aeruginosa* to repair random DNA cross-linkings upon photochemical treatment, leaving *P. aeruginosa* in a "killed but metabolically active" (KBMA) state without the ability to proliferate. Expression of the T3SS activator is controlled with an isopropyl β-d-1-thiogalactopyranoside-inducible promoter and major secreted exotoxins from the T3SS were deleted. To test the ability of KBMA *P. aeruginosa* T3SS to deliver functional proteins into eukaryotic cells, a signal peptide derived from exotoxin S (S54) was fused with β-lactamase and detectable β-lactamase activity in HL60 cells can be observed after incubating HL60 cells with KBMA *P. aeruginosa* for 3 h. Toxicity of the *P. aeruginosa* vaccine towards C57BL/6J mice showed that KBMA *P. aeruginosa* secreting antigen S54-OVA caused no mouse death while the live *P. aeruginosa* secreting S54-OVA killed all the mice within 24 h. KBMA *P. aeruginosa* secreting S54-OVA successfully disseminates into lymph nodes to activate dendritic cells for presenting antigens to CD8+ T cells, achieving efficient tumor protection in mice model xenografted with B16-OVA cells.

6.2 Human cells

In addition to bacteria, human derived cell lines were also developed as protein carriers with reduced concern about unexpected toxicity or immunogenicity as in bacterial carriers. Kown *et al.* utilized the long life-span of erythrocytes and translocated L-asparaginase into red blood cells (RBCs) *via* a protamine-asparaginase fusion to treat acute lymphoblastic leukemia.[123] The asparaginase loaded RBCs retained their native morphology as observed by scanning electron microscopy and shielded asparaginase from proteolytic degradation. In a lymphoma cell L5178Y bearing mice model, mice treated with asparaginase containing RBC elongated the mice survival time by ~44% as compared to the saline control group. Mitchell *et al.* coated leukocytes with TRAIL through E-selectin based adhesion to mimic natural killer cells for killing circulating cancer cells (CTC) in the bloodstream (**Figure 9**).[32] Leukocytes share similar migration characteristics with CTC in the near-wall region of bloodstreams due to the sialylated carbohydrate ligands presented on their surfaces that can interact with selectins on endothelial cell walls. The authors reasoned that functionalizing leukocytes with TRAIL could utilize the number advantage of leukocytes (leukocyte/CTC number ratio at ~ 1×10^6) to squeeze TRAIL onto the surface of sparse CTC (1-100 cells/mL) during migration. TRAIL was coated onto blood leukocytes *via* a liposome displaying both E-selectin and TRAIL under shear flow and the adhesion efficiency in leukocyte subpopulations were directly related with their E-selectin ligand expression levels. Liposome containing E-selectin injected into mice blood circulation readily adsorbed onto leukocytes, the injection of COLO 205 cells 30 min after E-selectin liposome or E-selectin/TRAIL liposome administration resulted in ~130,000 and <2000 living COLO 205 cells, respectively, confirming the anticancer effect of TRAIL coated leukocytes. Instead of using a liposome-assisted TRAIL displaying technique, Barti-Juhasz genetically engineered bone marrow derived mesenchymal stem/stromal cells (MSC) to express and secrete TRAIL from a transduced pORF-TRAIL plasmid.[124] *In vitro* tests showed that MSC-TRAIL inhibited the growth of RD rhabdomyosarcoma cells by 85%, while a MSC expressing GFP showed no significant inhibition.

The migratory ability and tumor tropism of stem cells make them attractive carriers for targeted cancer therapeutic delivery. Neural stem cells (NSCs), which can home in on tumors inside or outside the brain, was utilized by Zhu *et al.* to deliver a fusogenic membrane glycoprotein that can induce cell-to-cell fusion based cell death.[125] The vesicular stomatitis virus glycoprotein (VSV-G) is one of the fusogenic glycoproteins that mediates cell fusion at acid environment (pH 4.8 - pH 6.4). By introducing a point mutation H162R, the authors enhanced the working pH of VSV-G to pH 6.8, which matched extracellular pH at tumor tissue (pH 6.5 - pH 7.1) but below the pH of normal tissue (pH 7.3 - pH 7.4), leading to higher specificity towards tumor tissues. Immunofluorescence staining showed that both VSV-G wild type (WT) and H162R expressed from a recombinant plasmid in NSCs were successfully exported to cell surface. Incubating mouse 4T1 breast cancer cells with NSCs expressing WT or H162R at different pH shock conditions showed that no cell fusion occurred at pH 7.4 for both WT and H162R while cell fusion occurred at pH 6.8 for H162R but not WT. Combination of the pH selectivity of H162R and tumor tropism of NSCs showed enhanced specificity and tumor suppression effects in 4T1 cell-bearing mice *via* systemic administration, enhancing the median survival time from 17 days in the PBS

group to 24 days, while no significant off-target damage was detected in non-targeted organs.

7. Summary and outlook

Anticancer proteins, whether bind extracellular receptors or target intracellular machineries hold vast promise for cancer treatment. Substantial achievements have been made in tailoring carriers to protect fragile proteins against detrimental physiological environments and deliver the cargo proteins to their functional sites. As summarized in **Table 1**, various types of carriers, from inorganic particles to organic polymer capsules, and from synthetic particles to whole living cells, were developed to convoy therapeutic proteins to their targeting loci through local or systemic administration. Abundant experiences about efficient protein loading, uptake, release and targeting were accumulated. Despite these accomplishments, anticancer protein delivery is still in its infancy with only a few formulations made it through clinical trials and finally entered the market.[126]

Further optimizations of the carriers are needed with respect to their stability, biocompatibility and targeting efficiency. Combining the innate advantages of different carriers is a facile approach to develop more bio-compatible carriers. For example, to overcome the poor degradability of gold nanoparticles, degradable DNA can be incorporated into a gold nanoparticle matrix for enhanced elimination.[37] To improve tumor targeting efficiency of a polymeric nanoparticle, a tumor cell membrane derived lipid shell was coated onto the nanoparticle to formulate a biomimetic particle that can induce homotypic binding based targeting as well as cancer specific immune responses.[127] The concept of developing biomimetic carriers by using synthetic particles to mimic the functions of natural protein delivery carriers, such as viruses, bacteria, eukaryotic cells or cell compartments, is an effective strategy to deliver anticancer proteins.[43] Combination therapy is another effective cancer killing strategy by programing different anticancer therapeutics, such as protein, siRNA or small molecule drugs, inside one single carrier, activating different tumor inhibition pathways simultaneously.[10, 128, 129] In addition, adding stimuli responsiveness to protein carriers can reduce unexpected cytotoxicity. Off-target cytotoxicity caused by passive protein release can be reduced by spatial- temporal- and dosage- controllable drug release profiles. Endogenous characteristics of tumor tissue microenvironment (such as acid pH[130], high GSH concentration[131], high ATP concentration[132, 133] and overexpressed proteases[90]) and controllable external signals (such as temperature[134], electric/magnetic field[135, 136], ultrasound[137] or light[138]) can all be harnessed to achieve controlled protein release.[38] Although current protein delivery platforms mostly target primary tumors, with increasing understanding of tumor physiology carriers that combat metastatic tumors, which are generally considered incurable, at each stage of the metastasis can be expected.[139] Moreover, proteins can be utilized as versatile carriers for various kinds of drugs such as siRNA[140] or small molecule drugs[132, 133] for anticancer therapy. Drug loading and release profiles can be adjusted by tuning the surface properties of protein [141].

Last but no least, the added functionalities to protein delivery carriers, such as targeting ligand, stimuli sensors or other auxiliary moieties, for improved protein delivery efficacy, inevitably increase the synthesis complexity and cost of these formulations. The cost/benefit

ratio of adding these functions need to be considered for more competitive drugs in the future market.[142]

Acknowledgements

Biographies
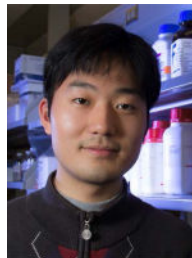
Wujin Sun received his B.S. degree in Bioengineering in 2010, followed by a M.S. degree in Biochemical Engineering from Nanjing University of Technology. He is currently a PhD student in Professor Zhen Gu's laboratory in the Joint Department of Biomedical Engineering at the University of North Carolina at Chapel Hill and North Carolina University, focusing on using biomacromolecules for drug delivery.

Yue Lu received her B.S. degree in Chemistry in 2012 from Nanjing University. She is currently a PhD student in Prof. Zhen Gu's research group in the Joint Department of Biomedical Engineering at the University of North Carolina at Chapel Hill and North Carolina University. Her current research interests include stimuli-responsive nanomaterials for anticancer drug delivery and diabetes therapy.

Zhen Gu received his B.S. degree in Chemistry and M.S. degrees in Polymer Chemistry and Physics from Nanjing University. In 2010, he obtained Ph.D. degree at the University of California, Los Angeles, under the guidance of Prof. Yi Tang in the Department of Chemical and Biomolecular Engineering. He was a postdoctoral associate working with Prof. Robert Langer at Massachusetts Institute of Technology and Harvard Medical School during 2010 to 2012. He is currently an Assistant Professor in the Joint Department of Biomedical Engineering at the University of North Carolina at Chapel Hill and North Carolina State University. He also holds a joint position in the UNC Eshelman School of Pharmacy. His group studies controlled drug delivery, bio-inspired materials and nanobiotechnology.

References

1. Peer D, Karp JM, Hong S, Farokhzad OC, Margalit R, Langer R. Nat. Nanotechnol. 2007; 2:751. [PubMed: 18654426]

2. Markman JL, Rekechenetskiy A, Holler E, Ljubimova JY. Adv. Drug Del. Rev. 2013; 65:1866.

3. Chen Y, Gao D-Y, Huang L. Adv. Drug Del. Rev. 2014 DOI: 10.1016/j.addr.2014.05.009.

4. Vermonden T, Censi R, Hennink WE. Chem. Rev. 2012; 112:2853. [PubMed: 22360637]

5. Hemler ME. Nat. Rev. Cancer. 2014; 14:49. [PubMed: 24505619]

6. Gu Z, Biswas A, Zhao M, Tang Y. Chem. Soc. Rev. 2011; 40:3638. [PubMed: 21566806]

7. Noteborn MH. Eur. J. Pharmacol. 2009; 625:165. [PubMed: 19836376]

8. Mocellin S, Rossi CR, Pilati P, Nitti D. Cytokine Growth F. R. 2005; 16:35.

9. Scott AM, Wolchok JD, Old LJ. Nat. Rev. Cancer. 2012; 12:278. [PubMed: 22437872]

10. Jiang T, Mo R, Bellotti A, Zhou J, Gu Z. Adv. Funct. Mater. 2013:2259.

11. Johnstone RW, Frew AJ, Smyth MJ. Nat. Rev. Cancer. 2008; 8:782. [PubMed: 18813321]

12. Kluck RM, Bossy-Wetzel E, Green DR, Newmeyer DD. Science. 1997; 275:1132. [PubMed: 9027315]

13. Stennicke HR, Salvesen GS. J. Biol. Chem. 1997; 272:25719. [PubMed: 9325297]

14. Samejima K, Earnshaw WC. Nat. Rev. Mol. Cell. Biol. 2005; 6:677. [PubMed: 16103871]

15. Mathas S, Rickers A, Bommert K, Dörken B, Mapara MY. Cancer Res. 2000; 60:7170. [PubMed: 11156427]

16. Sliwkowski MX, Mellman I. Science. 2013; 341:1192. [PubMed: 24031011]

17. Senzer N, Nemunaitis J, Nemunaitis D, Bedell C, Edelman G, Barve M, Nunan R, Pirollo KF, Rait A, Chang EH. Mol. Ther. 2013; 21:1096. [PubMed: 23609015]

18. Danen-van Oorschot AAAM, Zhang Y-H, Leliveld SR, Rohn JL, Seelen MCMJ, Bolk MW, van Zon A, Erkeland SJ, Abrahams J-P, Mumberg D, Noteborn MHM. J. Biol. Chem. 2003; 278:27729. [PubMed: 12754198]

19. Zhao M, Hu B, Gu Z, Joo K-I, Wang P, Tang Y. Nano Today. 2013; 8:11.

20. Tennant DA, Duran RV, Gottlieb E. Nat. Rev. Cancer. 2010; 10:267. [PubMed: 20300106]

21. Cohen JA, Beaudette TT, Tseng WW, Bachelder EM, Mende I, Engleman EG, Frechet JM. Bioconjug. Chem. 2009; 20:111. [PubMed: 19102625]

22. Kroemer G, Galluzzi L, Kepp O, Zitvogel L. Annu. Rev. Immunol. 2013; 31:51. [PubMed: 23157435]

23. Foster S, Duvall CL, Crownover EF, Hoffman AS, Stayton PS. Bioconjug. Chem. 2010; 21:2205. [PubMed: 21043513]

24. Yuba E, Kono Y, Harada A, Yokoyama S, Arai M, Kubo K, Kono K. Biomaterials. 2013; 34:5711. [PubMed: 23639528]

25. McNulty S, Colaco CA, Blandford LE, Bailey CR, Baschieri S, Todryk S. Immunology. 2013; 139:407. [PubMed: 23551234]

26. Hemmerle T, Neri D. Int. J. Cancer. 2014; 134:467. [PubMed: 23818211]

27. Lasek W, Zago d on R, Jakobisiak M. Cancer Immunol. Immunother. 2014; 63:1. [PubMed: 23955682]

28. De Groot AS, Martin W. Clin. Immunol. 2009; 131:189. [PubMed: 19269256]

29. Zhao M, Biswas A, Hu B, Joo K-I, Wang P, Gu Z, Tang Y. Biomaterials. 2011; 32:5223. [PubMed: 21514660]

30. Zhang Y, Chan HF, Leong KW. Adv. Drug Del. Rev. 2013; 65:104.

31. Bernardes N, Chakrabarty A, Fialho A. Appl. Microbiol. Biotechnol. 2013; 97:5189. [PubMed: 23644748]

32. Mitchell MJ, Wayne E, Rana K, Schaffer CB, King MR. Proc. Natl. Acad. Sci. U. S. A. 2014 DOI: 10.1073/pnas.1316312111.

33. Su W, Wang L, Zhou M, Liu Z, Hu S, Tong L, Liu Y, Fan Y, Kong D, Zheng Y, Han Z, Wu JC, Xiang R, Li Z. Cell Transplant. 2013; 22:2079. [PubMed: 23067802]

34. Kolesnikova TA, Skirtach AG, Möhwald H. Expert Opin. Drug Del. 2013; 10:47.

35. Danhier F, Feron O, Préat V. J. Control. Release. 2010; 148:135. [PubMed: 20797419]

36. Lu Y, Sun W, Gu Z. J. Control. Release. 2014 In Press.

37. Chou LYT, Zagorovsky K, Chan WCW. Nat. Nanotechnol. 2014; 9:148. [PubMed: 24463361]

38. Mura S, Nicolas J, Couvreur P. Nat. Mater. 2013; 12:991. [PubMed: 24150417]

39. Yoo J-W, Doshi N, Mitragotri S. Adv. Drug Del. Rev. 2011; 63:1247.

40. Kim TH, Jiang HH, Park CW, Youn YS, Lee S, Chen X, Lee KC. J. Control. Release. 2011; 150:63. [PubMed: 21062635]

41. Mundargi RC, Babu VR, Rangaswamy V, Patel P, Aminabhavi TM. J. Control. Release. 2008; 125:193. [PubMed: 18083265]

42. He H, Ye J, Wang Y, Liu Q, Chung HS, Kwon YM, Shin MC, Lee K, Yang VC. J. Control. Release. 2014; 176:123. [PubMed: 24374002]

43. Yoo J-W, Irvine DJ, Discher DE, Mitragotri S. Nat. Rev. Drug Discov. 2011; 10:521. [PubMed: 21720407]

44. Malmsten M. Curr. Opin. Colloid In. 2013; 18:468.

45. Kim CS, Tonga GY, Solfiell D, Rotello VM. Adv. Drug Del. Rev. 2013; 65:93.

46. Epple M, Ganesan K, Heumann R, Klesing J, Kovtun A, Neumann S, Sokolova V. J. Mater. Chem. 2010; 20:18.

47. Wu X, Song Y, Han J, Yang L, Han S. Biomater. Sci. 2013; 1:918.

48. Kanwar JR, Mahidhara G, Kanwar RK. Nanomedicine. 2012; 7:1521. [PubMed: 22734611]

49. Sahdev P, Podaralla S, Kaushik RS, Perumal O. J. Biomed. Nanotechnol. 2013; 9:132. [PubMed: 23627076]

50. De Volder MFL, Tawfick SH, Baughman RH, Hart AJ. Science. 2013; 339:535. [PubMed: 23372006]

51. Cheng Q, Blais M-O, Harris G, Jabbarzadeh E. PLoS ONE. 2013; 8:e81947. [PubMed: 24312611]

52. Calvaresi M, Zerbetto F. Acc. Chem. Res. 2013; 46:2454. [PubMed: 23826731]

53. Li C, Bolisetty S, Chaitanya K, Adamcik J, Mezzenga R. Adv. Mater. 2013; 25:1010. [PubMed: 23135812]

54. Weng X, Wang M, Ge J, Yu S, Liu B, Zhong J, Kong J. Mol. Biosyst. 2009; 5:1224. [PubMed: 19756312]

55. Wang M, Yu S, Wang C, Kong J. ACS Nano. 2010; 4:6483. [PubMed: 20977256]

56. Goenka S, Sant V, Sant S. J. Control. Release. 2014; 173:75. [PubMed: 24161530]

57. Koninti RK, Sengupta A, Gavvala K, Ballav N, Hazra P. Nanoscale. 2014; 6:2937. [PubMed: 24477816]

58. Shen H, Liu M, He H, Zhang L, Huang J, Chong Y, Dai J, Zhang Z. ACS Appl. Mater. Interfaces. 2012; 4:6317. [PubMed: 23106794]

59. Zhang Y, Petibone D, Xu Y, Mahmood M, Karmakar A, Casciano D, Ali S, Biris AS. Drug Metab. Rev. 2014; 46:232. [PubMed: 24506522]

60. Mahony D, Cavallaro AS, Stahr F, Mahony TJ, Qiao SZ, Mitter N. Small. 2013; 9:3138. [PubMed: 23625779]

61. Mody KT, Popat A, Mahony D, Cavallaro AS, Yu C, Mitter N. Nanoscale. 2013; 5:5167. [PubMed: 23657437]

62. Gu J, Huang K, Zhu X, Li Y, Wei J, Zhao W, Liu C, Shi J. J. Colloid Interface Sci. 2013; 407:236. [PubMed: 23866201]

63. Méndez J, Morales Cruz M, Delgado Y, Figueroa CM, Orellano EA, Morales M, Monteagudo A, Griebenow K. Mol. Pharm. 2013; 11:102. [PubMed: 24294910]

64. Kumar A, Zhang X, Liang X-J. Biotechnol. Adv. 2013; 31:593. [PubMed: 23111203]

65. Tang R, Kim CS, Solfiell DJ, Rana S, Mout R, Velázquez-Delgado EM, Chompoosor A, Jeong Y, Yan B, Zhu Z-J, Kim C, Hardy JA, Rotello VM. ACS Nano. 2013; 7:6667. [PubMed: 23815280]

66. Ahn S, Lee I-H, Kang S, Kim D, Choi M, Saw PE, Shin E-C, Jon S. Adv. Healthcare Mater. 2014 DOI: 10.1002/adhm.201300597.

67. Huang Y, Yu F, Park Y-S, Wang J, Shin M-C, Chung HS, Yang VC. Biomaterials. 2010; 31:9086. [PubMed: 20828812]

68. Tang H, Kobayashi H, Niidome Y, Mori T, Katayama Y, Niidome T. J. Control. Release. 2013; 171:178. [PubMed: 23863449]

69. Allen TM, Cullis PR. Adv. Drug Del. Rev. 2013; 65:36.

70. Sarker SR, Hokama R, Takeoka S. Mol. Pharm. 2014; 11:164. [PubMed: 24224643]

71. De Miguel D, Basáñez G, Sánchez D, Malo PG, Marzo I, Larrad L, Naval J, Pardo J, Anel A, Martinez-Lostao L. Mol. Pharm. 2013; 10:893. [PubMed: 23331277]

72. Seifert O, Pollak N, Nusser A, Steiniger F, Rüger R, Pfizenmaier K, Kontermann RE. Bioconjugate Chem. 2014; 25:879.

73. Kim SK, Foote MB, Huang L. Biomaterials. 2012; 33:3959. [PubMed: 22365810]

74. Wang M, Alberti K, Sun S, Arellano CL, Xu Q. Angew. Chem. Int. Ed. 2014; 126:2937.

75. Guo L, Fan L, Ren J, Pang Z, Ren Y, Li J, Wen Z, Qian Y, Zhang L, Ma H, Jiang X. International journal of nanomedicine. 2012; 7:1449. [PubMed: 22619505]

76. Guo L, Fan L, Pang Z, Ren J, Ren Y, Li J, Chen J, Wen Z, Jiang X. J. Control. Release. 2011; 154:93. [PubMed: 21609741]

77. Yeo RWY, Lai RC, Zhang B, Tan SS, Yin Y, Teh BJ, Lim SK. Adv. Drug Del. Rev. 2013; 65:336.

78. El Andaloussi S, Mager I, Breakefield XO, Wood MJA. Nat. Rev. Drug Discov. 2013; 12:347. [PubMed: 23584393]

79. Gehrmann U, Hiltbrunner S, Georgoudaki AM, Karlsson MC, Naslund TI, Gabrielsson S. Cancer Res. 2013; 73:3865. [PubMed: 23658368]

80. Tian X, Zhu M, Tian Y, Ramm GA, Zhao Y, Nie G. Biomaterials. 2012; 33:6147. [PubMed: 22681975]

81. Mizrak A, Bolukbasi MF, Ozdener GB, Brenner GJ, Madlener S, Erkan EP, Strobel T, Breakefield XO, Saydam O. Mol. Ther. 2013; 21:101. [PubMed: 22910294]

82. Roberts MJ, Bentley MD, Harris JM. Adv. Drug Del. Rev. 2012; 64:116.

83. Alconcel SNS, Baas AS, Maynard HD. Polym. Chem. 2011; 2:1442.

84. Chen J, Zhao M, Feng F, Sizovs A, Wang J. J. Am. Chem. Soc. 2013; 135:10938. [PubMed: 23848502]

85. Murata H, Sakaguchi M, Futami J, Kitazoe M, Maeda T, Doura H, Kosaka M, Tada H, Seno M, Huh NH, Yamada H. Biochemistry. 2006; 45:6124. [PubMed: 16681385]

86. Keefe AJ, Jiang S. Nat. Chem. 2012; 4:59. [PubMed: 22169873]

87. Ding H, Helguera G, Rodríguez JA, Markman J, Luria-Pérez R, Gangalum P, Portilla-Arias J, Inoue S, Daniels-Wells TR, Black K, Holler E, Penichet ML, Ljubimova JY. J. Control. Release. 2013; 171:322. [PubMed: 23770212]

88. Gu Z, Yan M, Hu B, Joo K-I, Biswas A, Huang Y, Lu Y, Wang P, Tang Y. Nano Lett. 2009; 9:4533. [PubMed: 19995089]

89. Gu Z, Biswas A, Joo KI, Hu B, Wang P, Tang Y. Chem. Commun. 2010; 46:6467.

90. Biswas A, Joo K-I, Liu J, Zhao M, Fan G, Wang P, Gu Z, Tang Y. ACS Nano. 2011; 5:1385. [PubMed: 21268592]

91. Li N, Peng L-H, Chen X, Zhang T-Y, Shao G-F, Liang W-Q, Gao J-Q. Nanomed. Nanotechnol. Biol. Med. 2014; 10:215.

92. Noh Y-W, Jang Y-S, Ahn K-J, Lim YT, Chung BH. Biomaterials. 2011; 32:6254. [PubMed: 21620470]

93. Sarti F, Perera G, Hintzen F, Kotti K, Karageorgiou V, Kammona O, Kiparissides C, Bernkop-Schnürch A. Biomaterials. 2011; 32:4052. [PubMed: 21377204]

94. Azagarsamy MA, Alge DL, Radhakrishnan SJ, Tibbitt MW, Anseth KS. Biomacromolecules. 2012; 13:2219. [PubMed: 22746981]

95. Kesharwani P, Jain K, Jain NK. Prog. Polym. Sci. 2014; 39:268.

96. Sheng K-C, Kalkanidis M, Pouniotis DS, Esparon S, Tang CK, Apostolopoulos V, Pietersz GA. Eur. J. Immunol. 2008; 38:424. [PubMed: 18200633]

97. Ng DYW, Arzt M, Wu Y, Kuan SL, Lamla M, Weil T. Angew. Chem. Int. Ed. 2014; 53:324.

98. Ng DYW, Fahrer J, Wu Y, Eisele K, Kuan SL, Barth H, Weil T. Adv. Healthcare Mater. 2013; 2:1620.

99. Lee JS, Feijen J. J. Control. Release. 2012; 161:473. [PubMed: 22020381]

100. Scott EA, Stano A, Gillard M, Maio-Liu AC, Swartz MA, Hubbell JA. Biomaterials. 2012; 33:6211. [PubMed: 22658634]

101. Wang X, Sun H, Meng F, Cheng R, Deng C, Zhong Z. Biomacromolecules. 2013; 14:2873. [PubMed: 23815094]

102. Cheng R, Meng F, Ma S, Xu H, Liu H, Jing X, Zhong Z. J. Mater. Chem. 2011; 21:19013.

103. Tai W, Mo R, Lu Y, Jiang T, Gu Z. Biomaterials. 2014; 35:7194. [PubMed: 24875756]

104. Lee Y, Ishii T, Cabral H, Kim HJ, Seo JH, Nishiyama N, Oshima H, Osada K, Kataoka K. Angew. Chem. Int. Ed. Engl. 2009; 48:5309. [PubMed: 19294716]

105. Ren J, Zhang Y, Zhang J, Gao H, Liu G, Ma R, An Y, Kong D, Shi L. Biomacromolecules. 2013; 14:3434. [PubMed: 24063314]

106. Keller S, Wilson JT, Patilea GI, Kern HB, Convertine AJ, Stayton PS. J. Control. Release. 2014

107. Zhang Z, Eckert MA, Ali MM, Liu L, Kang D-K, Chang E, Pone EJ, Sender LS, Fruman DA, Zhao W. ChemBioChem. 2014:1268. [PubMed: 24803415]

108. Liu X, Xu Y, Yu T, Clifford C, Liu Y, Yan H, Chang Y. Nano Lett. 2012; 12:4254. [PubMed: 22746330]

109. Erben CM, Goodman RP, Turberfield AJ. Angew. Chem. Int. Ed. 2006; 45:7414.

110. Douglas SM, Bachelet I, Church GM. Science. 2012; 335:831. [PubMed: 22344439]

111. Wang F, Wang Y, Zhang X, Zhang W, Guo S, Jin F. J. Control. Release. 2014; 174:126. [PubMed: 24291335]

112. Granadillo M, Vallespi MG, Batte A, Mendoza O, Soria Y, Lugo VM, Torrens I. Vaccine. 2011; 29:920. [PubMed: 21145912]

113. Essafi M, Baudot AD, Mouska X, Cassuto J-P, Ticchioni M, Deckert M. Mol. Cancer Ther. 2011; 10:37. [PubMed: 21220490]

114. Teicher BA, Chari RVJ. Clin. Cancer Res. 2011; 17:6389. [PubMed: 22003066]

115. Bull-Hansen B, Cao Y, Berg K, Skarpen E, Rosenblum MG, Weyergang A. J. Control. Release. 2014; 182:58. [PubMed: 24637464]

116. Tran M, Van C, Barrera DJ, Pettersson PL, Peinado CD, Bui J, Mayfield SP. Proc. Natl. Acad. Sci. U. S. A. 2013; 110:E15. [PubMed: 23236148]

117. Schoonen L, van Hest JCM. Nanoscale. 2014; 6:7124. [PubMed: 24860847]

118. Patel KG, Swartz JR. Bioconjugate Chem. 2011; 22:376.

119. Wörsdörfer B, Pianowski Z, Hilvert D. J. Am. Chem. Soc. 2011; 134:909. [PubMed: 22214519]

120. Forbes NS. Nat. Rev. Cancer. 2010; 10:785. [PubMed: 20944664]

121. Zhu C, Yang Q, Lv F, Liu L, Wang S. Adv. Mater. 2013; 25:1203. [PubMed: 23280674]

122. Le Gouellec A, Chauchet X, Laurin D, Aspord C, Verove J, Wang Y, Genestet C, Trocme C, Ahmadi M, Martin S, Broisat A, Cretin F, Ghezzi C, Polack B, Plumas J, Toussaint B. Mol. Ther. 2013; 21:1076. [PubMed: 23531551]

123. Kwon YM, Chung HS, Moon C, Yockman J, Park YJ, Gitlin SD, David AE, Yang VC. J. Control. Release. 2009; 139:182. [PubMed: 19577600]

124. Barti-Juhasz H, Mihalik R, Nagy K, Grisendi G, Dominici M, Petak I. Haematologica. 2011; 96:e21. [PubMed: 21357712]

125. Zhu D, Lam DH, Purwanti YI, Goh SL, Wu C, Zeng J, Fan W, Wang S. Mol. Ther. 2013; 21:1621. [PubMed: 23752308]

126. Venditto VJ, Szoka FC Jr. Adv. Drug Del. Rev. 2013; 65:80.

127. Fang RH, Hu C-MJ, Luk BT, Gao W, Copp JA, Tai Y, O'Connor DE, Zhang L. Nano Lett. 2014; 14:2181. [PubMed: 24673373]

128. Vanneman M, Dranoff G. Nat. Rev. Cancer. 2012; 12:237. [PubMed: 22437869]

129. Hu C-MJ, Zhang L. Biochem. Pharmacol. 2012; 83:1104. [PubMed: 22285912]

130. Ke C-J, Su T-Y, Chen H-L, Liu H-L, Chiang W-L, Chu P-C, Xia Y, Sung H-W. Angew. Chem. Int. Ed. 2011; 50:8086.

131. Ong W, Yang Y, Cruciano AC, McCarley RL. J. Am. Chem. Soc. 2008; 130:14739. [PubMed: 18841890]

132. Mo R, Jiang T, DiSanto R, Tai W, Gu Z. Nat. Commun. 2014; 5:3364. [PubMed: 24618921]

133. Mo R, Jiang T, Gu Z. Angew. Chem. Int. Ed. 2014:5925.

134. Choi S-W, Zhang Y, Xia Y. Angew. Chem. Int. Ed. 2010; 49:7904.

135. Oliveira H, Pérez-Andrés E, Thevenot J, Sandre O, Berra E, Lecommandoux S. J. Control. Release. 2013; 169:165. [PubMed: 23353805]

136. Kwon IC, Bae YH, Kim SW. Nature. 1991; 354:291. [PubMed: 1956379]

137. Di J, Price J, Gu X, Jiang X, Jing Y, Gu Z. Adv. Healthcare Mater. 2013; 3:811.

138. Zhang Y, Yin Q, Yin L, Ma L, Tang L, Cheng J. Angew. Chem. Int. Ed. 2013; 52:6435.

139. Schroeder A, Heller DA, Winslow MM, Dahlman JE, Pratt GW, Langer R, Jacks T, Anderson DG. Nat. Rev. Cancer. 2012; 12:39. [PubMed: 22193407]

140. Qi L, Wu L, Zheng S, Wang Y, Fu H, Cui D. Biomacromolecules. 2012; 13:2713.

141. Elzoghby AO, Samy WM, Elgindy NA. J. Control. Release. 2012:157.

142. Cheng Z, Al Zaki A, Hui JZ, Muzykantov VR, Tsourkas A. Science. 2012; 338:903. [PubMed: 23161990]
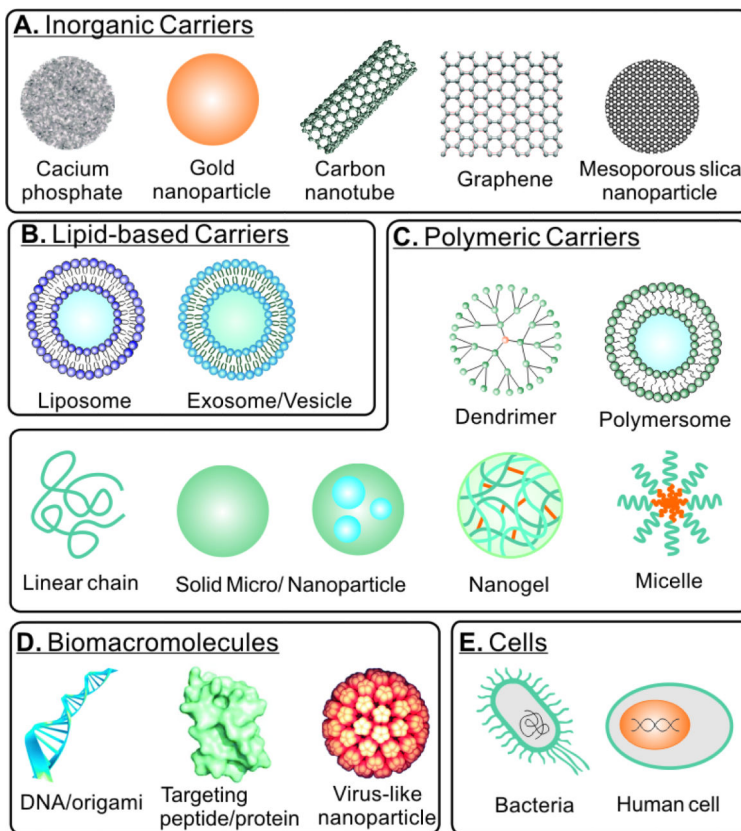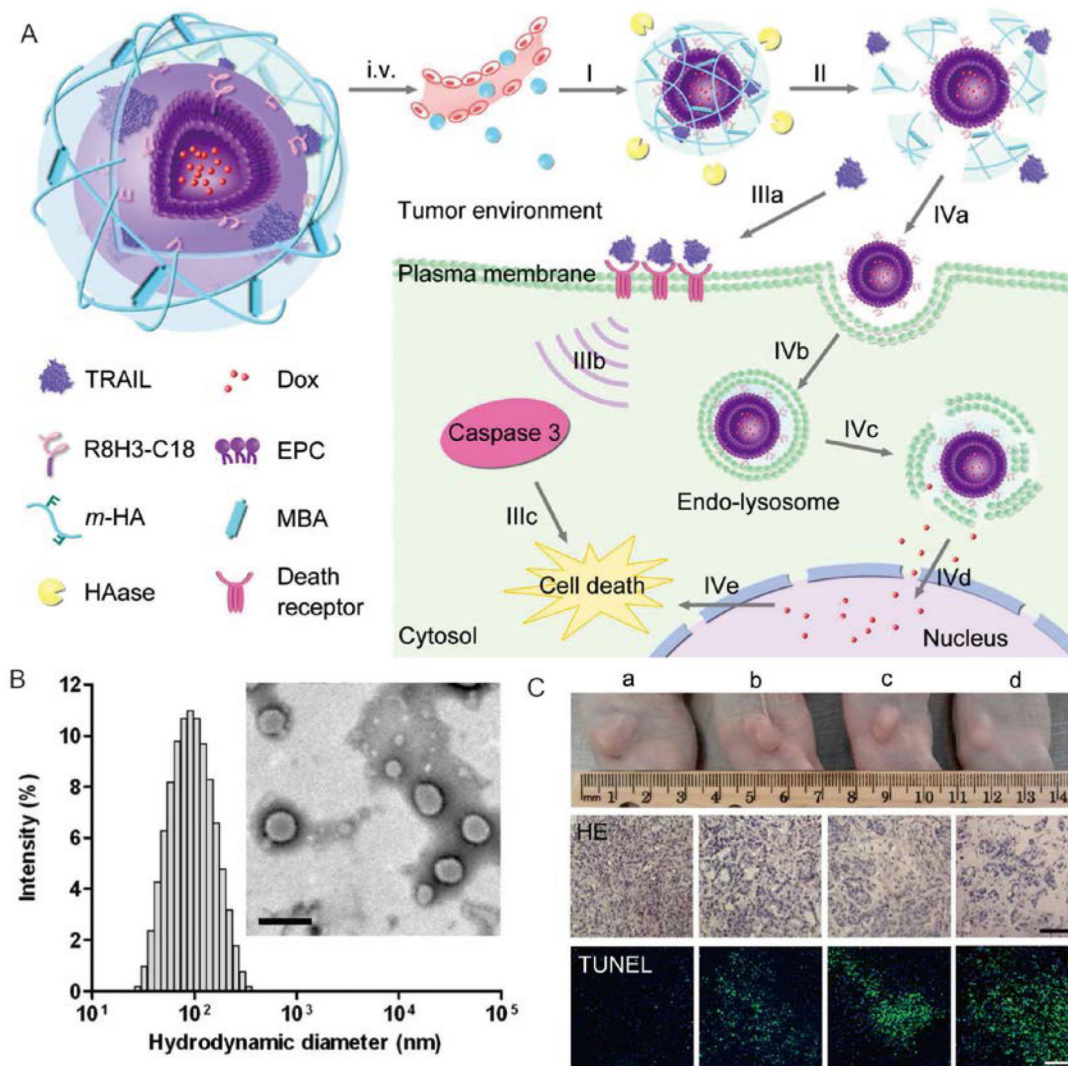
Figure 1.
Schematic of different carriers for anticancer protein delivery.
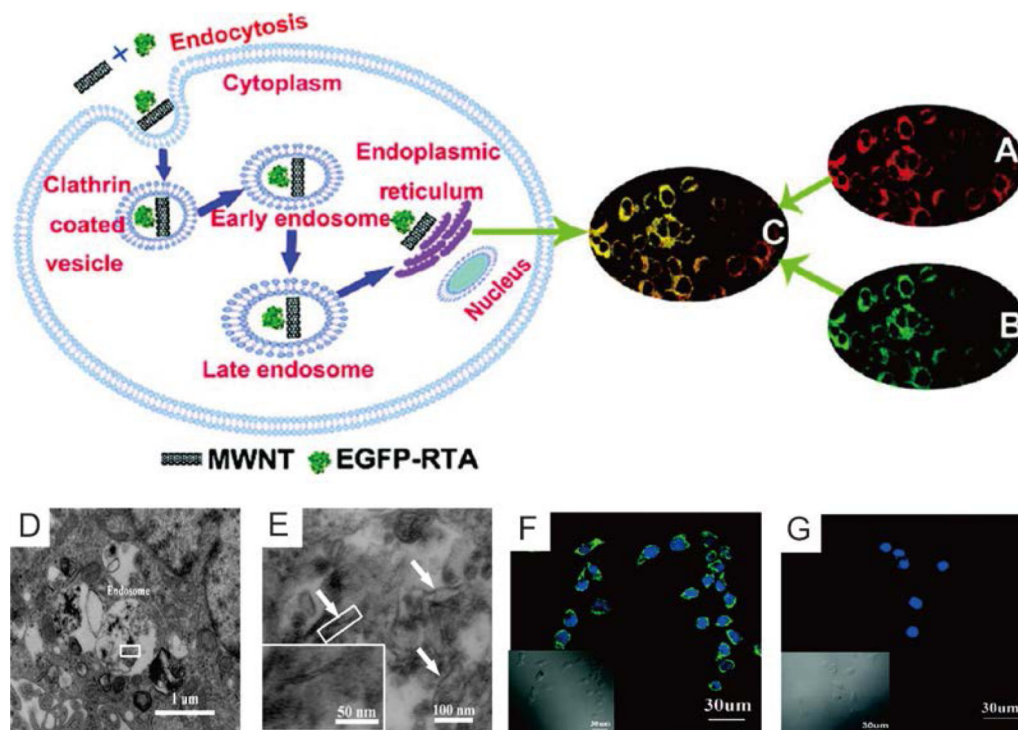
Figure 2.
Multiwall carbon nanotube (MWCNT) mediated intracellular delivery of ricin A-chain (RTA) through clathrin-mediated endocytosis by Kong and coworkers. (A) Confocal fluorescent image of endoplasmatic reticulum. (B) Confocal fluorescent image of EGFP-RTA. (C) Co-localization of EGFP-RTA with endoplasmatic reticulum. (D) TEM image of MWCNT localized in endosome and (E) Magnification of the white rectangular in D shows individual MWCNTs. (F) Confocal image of cells incubated with MWCNT-RTA conjugate and (G) Control confocal image of cells incubated with soluble RTA. Reprinted with permission from ref.[55]. Copyright 2010 American Chemical Society.
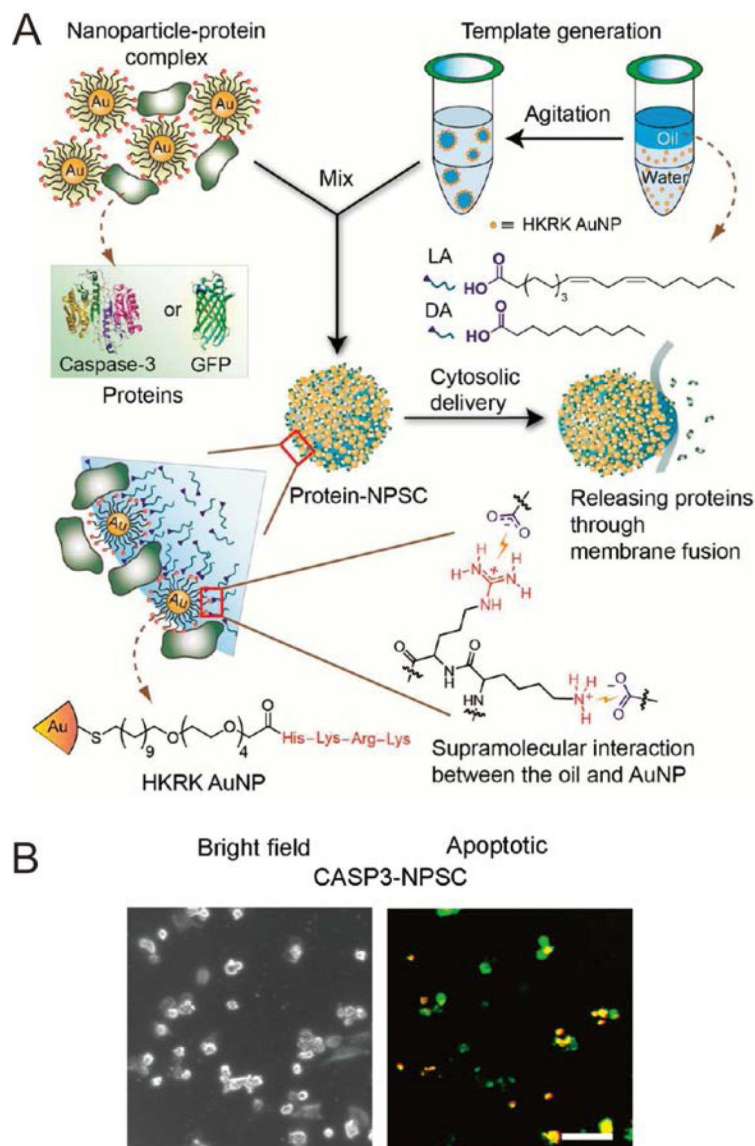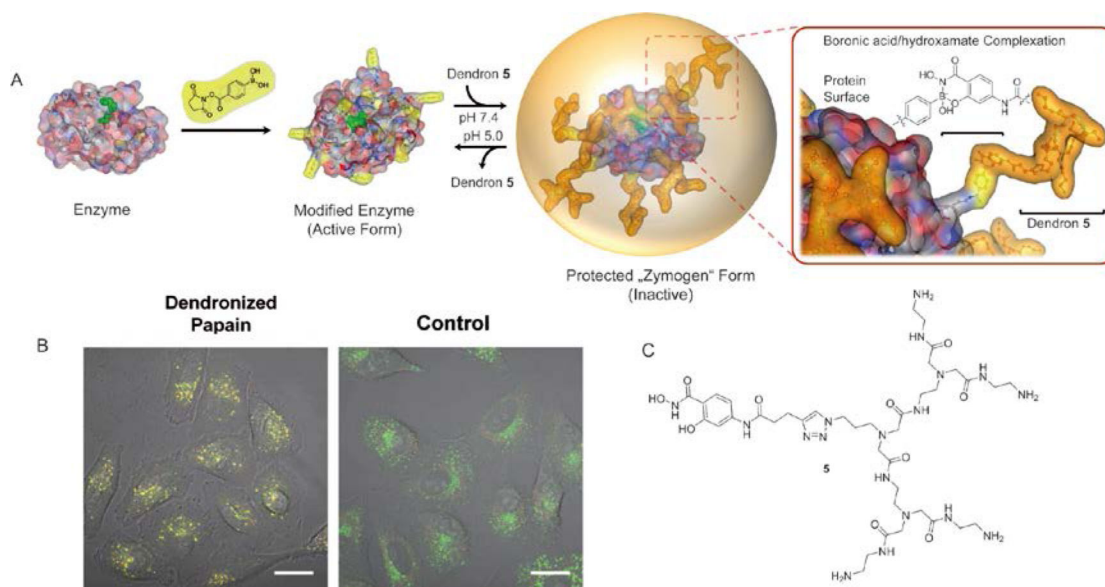
Figure 3.
Intracellular delivery of caspase 3 using nanoparticle stabilized capsules (NPSC) by Rotello and coworkers. (A) Schematic of the preparation of protein-NPSC complex and mechanism for protein delivery. (B) Delivery of caspase 3 into the cytosol of HeLa cells by caspase 3-NPSC complex. Copyright 2013 American Chemical Society.
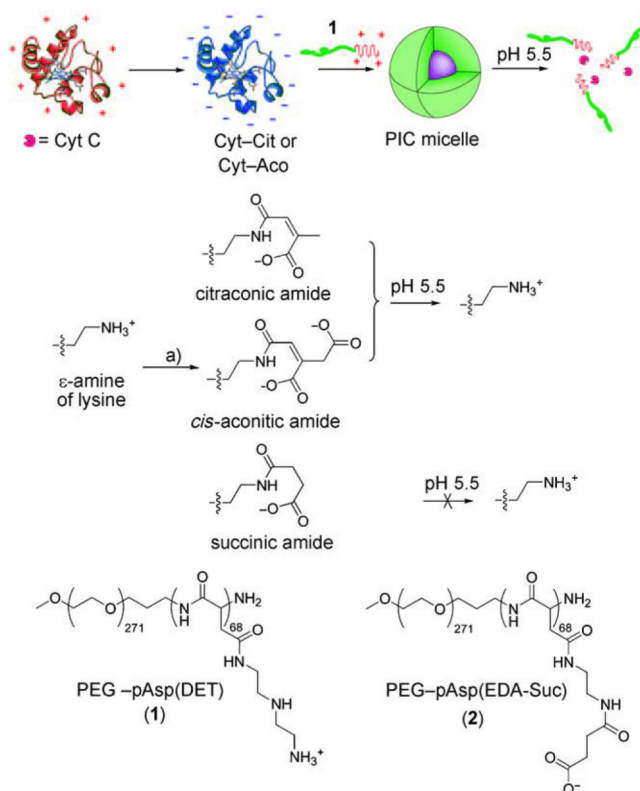
Figure 4.
Sequential delivery of TRAIL and Doxorubicin (DOX) to specific cellular locus using a polymeric gel coated liposome (Gelipo) by Gu and coworkers.[10] (A) Schematic of sequential deliveries of TRAIL to cell membrane and DOX to nucleus. I, TRAIL/DOX-Gelipo accumulated at tumor site by passive and active targeting. II, Degradation of the polymeric shell (HA) by overexpressed HAase at tumor site. IIIa, TRAIL was released and binds to the death receptors on cell surface. IIIb and IIIc, TRAIL induced apoptosis signaling and cell death. IVa and IVb, Liposome uptake mediated by surface modified R8H3 ligand. IVc and IVd, Endosome escape and release Dox into nucleus. IVe, Dox induced cell death. (B) Hydrodynamic size and TEM image of TRAIL/DOX-Gelipo. Scale bar 200 nm. (C) Mice bearing MDA-MB-231 xenograft treated with (a) Saline, (b) DOX solution, (c) DOX-Gelipo and (d) TRAIL/Dox-Gelipo. Reprinted with permission from ref.[10]. Copyright 2014 Wiley-VCH.
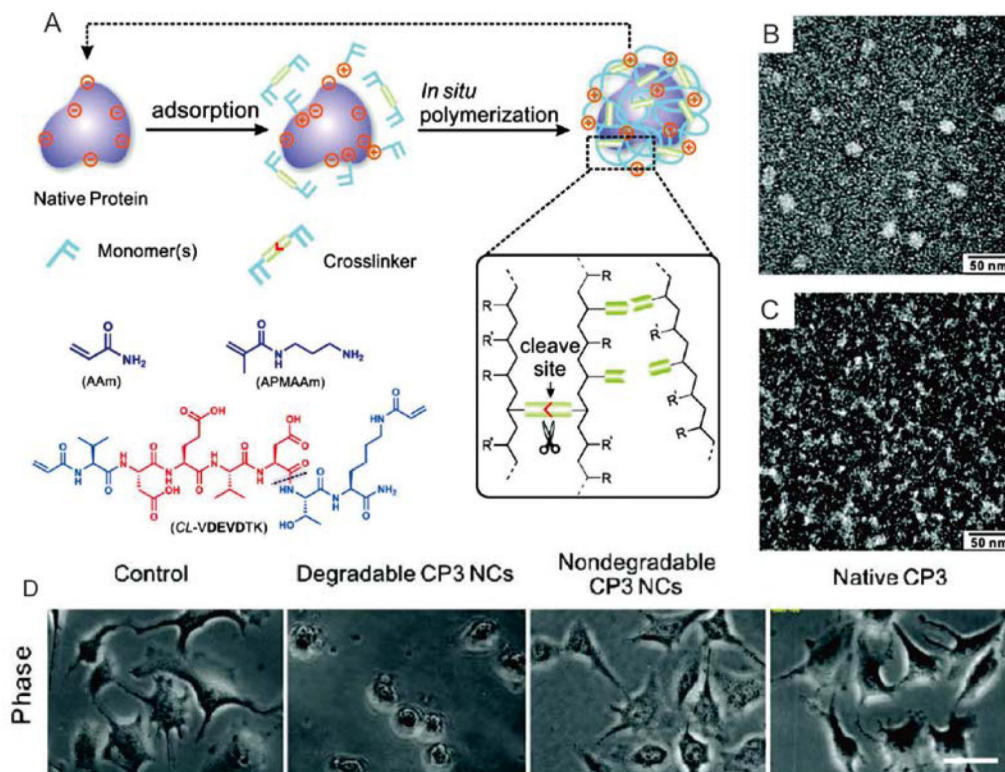
Figure 5.
Self-degradable single protein nano-capsule for delivering caspase 3 by Tang and coworkers. (A) Schematic diagram of the *in situ* polymerization process. (B) TEM characterization of freshly prepared caspase-3 capsule and (C) TEM image of self degradable caspase-3 capsule after incubation at 37 °C for 12h . (D) Bright field image of HeLa cells treated with saline, self-degradable caspase-3 capsule, non-degradable caspase-3 capsule and naked caspase-3 for 24 h. Reproduced with permission from ref.[88]. Copyright 2009 American Chemical Society.
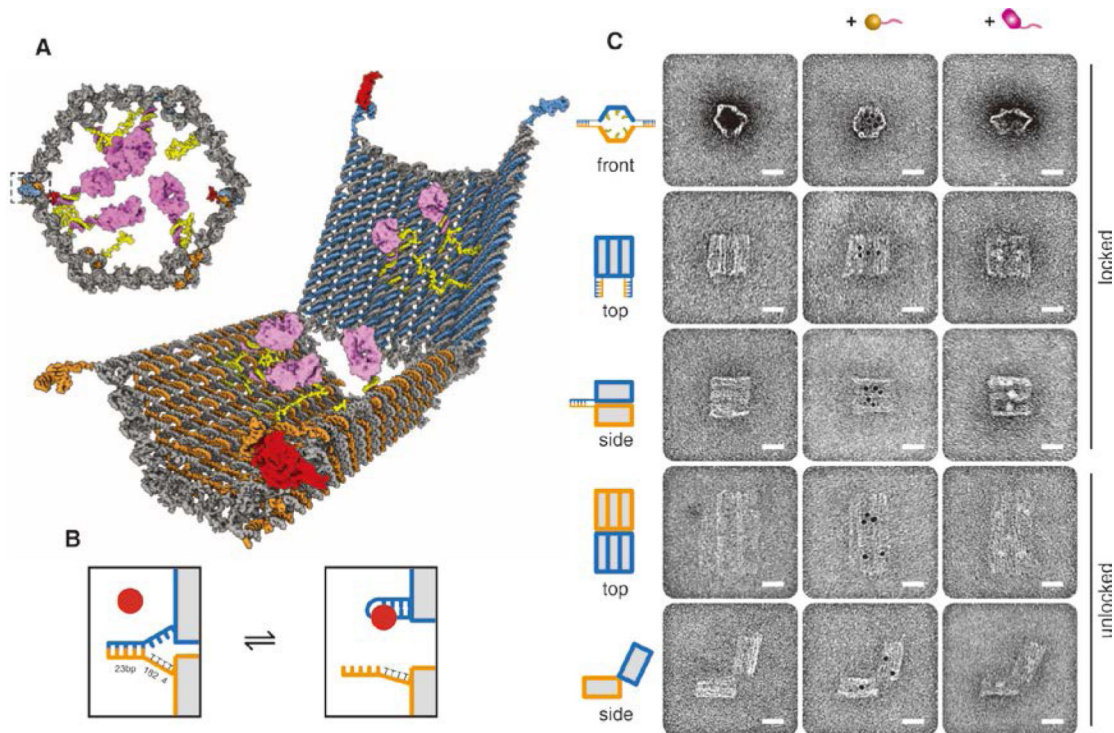
Figure 6.
Coating pH responsive dendritic shell on protein surface for intracellular delivery by Weil and coworkers. (A) Schematic diagram of the pH responsive dendritic coating and de-coating on protein surface. (B) Colocalization of dendronized papain and A549 cell lysosome. (C) Structure of the dendron. Reprinted with permission from ref.[97]. Copyright 2013 Wiley-VCH.
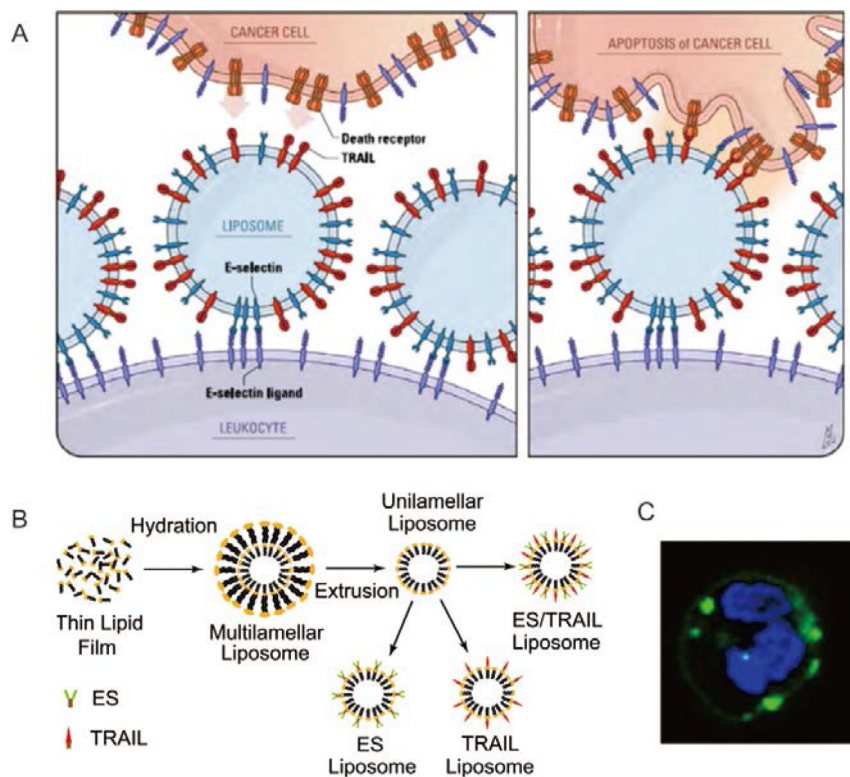
Figure 7.
Charge-conversional PIC micelles for delivering cytochrome *c* by Kataoka and Coworkers.
Schematic of the preparation of the PIC micelle. Copyright 2009 Wiley-VCH.

Figure 8.
Deliver antibodies with logic aptamer-gated nanorobot by Douglas and coworkers. (A) Schematic view the nanorobot in closed and open status. (B) Mechanism of the aptamer guided lock and open. Aptamer strand (blue), complementary strand to the aptamer (orange) and antigen (red). (C) TEM characterization of the open and close of nanorobot (left lane), nanorobot loaded with 5 nm gold nanoparticle (middle lane) and nanorobot loaded with antigen (right lane). Reprinted with permission from ref.[110]. Copyright 2012 Science.

Figure 9.
Coating TRAIL on leukocyte surface to target circulating tumor cells in bloodstream by King and coworkers. (A) Schematic diagram of liposome assisted coating of leukocytes with TRAIL and tumor targeting. (B) Schematic diagram of synthesizing liposomes containing TRAIL and E-selectin. (C) Confocal image of TRAIL coated leukocytes. Reproduced with permission from ref.[32]. Copyright 2014 PNAS.

Table 1

Summary of recent anticancer protein delivery carriers.

Types of carrier		Properties	Therapeutic proteins	cell lines	ref
Inorganic	Calcium phosphate	150-350 nm	Bovine pancreatic ribonuclease (RNAse), iron-saturated bovine lactoferrin (Fe-bLf), ovalbumin (OVA)	Caco-2 cells, HeLa, HepG2 L929 cells	[47-49]
	PEGylated graphene oxide	200nm width, 3.6 nm thickness, negatively charged	RNAse, proteinkinase A	HeLa and MCF-7	[58]
	Multiwalled carbon nanotubes	length 1-5μm, diameter 15-50 nm	Caspase-3, ricin A chain protein (RTA), anti-HER2	MG-63, L-929, HL7702, MCF-7, HeLa and COS-7	[51, 54, 55]
	Mesoporous silica nanoparticles	diameter 90-150 nm, pore size 3.6-4.5 nm	OVA, cytochrome c	HeLa	[60, 62]
	Gold nanoparticles	5 -140 nm	Caspase 3, OVA, extra domain B (EDB) of fibronectin-OVA$_{257-269}$	Hela CCD 1106 KERTr, DC2.4	[65-67]
Lipid	Liposome	~60-180 nm	OVA, TRAIL, anti-EGFR	MDA-MB-231, U87MG, colo 205, Jurkat, DC2.4	[10, 24, 71, 72, 76]
	Exosome/vescicle	30-160 nm	OVA, cytosine deaminase (CD) fused to uracil phosphoribosyltransferase (UPRT), tumor cell specific antigen	B16/OVA, schwannomas, B16, Lewis lung carcinoma (LLC)	[79-81]
polymer	PEGylation		TRAIL	Jurkat	[84]
	PEI conjugation		p53	Saos-2	[85]
	Polymalic acid conjugation	27 nm	Interleukin-2 fused with anti-HER2/neu	D2F2,BT-474,SK-BR-3,	[87]
	Single protein capsules	9 nm - 36nm, positively charged	Klf4, caspase-3, apoptin	MDA-MB-231, HeLa, MCF-7, U-87 MG	[19, 29, 88, 90]
	Crosslinked chitosan nanoparticle	~258 nm, positively charged	OVA, gp100	B16BL6	[91]
	PLGA particles by double emulsion	200 nm - 13μm, negatively charged	TRAIL, OVA	HCT 116, EG7-OVA	[40, 92, 93]
	Polyamidoamine based dendrimer	~ 7 nm	OVA, p53, cytochrome c, trypsin, papain, DNase I	B16-OVA, HeLa, A549, SaOS	[96-98]
	polymersome	100 nm -200 nm	OVA, cytochrome c, granzyme B	DC, CD8$^+$ T cells, HepG2, HeLa and MCF-7 cells	[100-102]
	polymeric micelle	25-85 nm	Cytochrome c, OVA	HepG2, MCF7, DC 2.4	[105, 106]
Biomacromolecules	Linear DNA conjugation	Negatively charged	Anti-CD-20	CCRF-CEM, Jurkat, and Ramos cells	[107]
	DNA nanostructure	Negatively charged	Streptavidin, cytochrome c, anti-(HLA)–A/B/C anti- CD33, anti-CDw328 Fab' fragments, anti- flagellin Fab'	RAW 264.7, Ramos, Kasumi-1, NKL	[108-110]
	Cell penetrating peptide conjugation		FOXO3 mutant, human papillomavirus (HPV) 16 E7 antigen	Jurkat, Raji, RPMI 8866, SKW6.4, U937 and K562, EHEB, H-2^b, TC-1, J774, CRL-1550	[112, 113]
	Antibody conjugation		Anti-HER2, anti -CD22, gelonin, exotoxin A	MDA-MB-231, BT-20, Zr-75-1, SK-BR-3,	[115, 116]

Types of carrier		Properties	Therapeutic proteins	cell lines	ref
				CA-46, Ramos, and Jurkat cells	
	Virus like protein particle		Idiotypic antibody fused with macrophage-colony stimulating factor	NFS-60	[118]
Cell	Bacteria based human cell based	1-3 μm	β-lactamase (Bla), OVA, exotoxin A	HL60, B16-OVA, A498	[121, 122]
			L-Asparaginase, TRAIL, stomatitis virus glyco-protein (VSV-G) H162R	L5178Y, COLO 205, PC-3, 4T1, Rhabdomyosarcoma	[32, 123-125]